



Raytheon

AEROSOL OPTICAL THICKNESS AND PARTICLE SIZE PARAMETER VISIBLE/INFRARED IMAGER/RADIOMETER SUITE ALGORITHM THEORETICAL BASIS DOCUMENT

Version 3: May 2000

Heather Kilcoyne
Doug Hoyt
Tom Zhao
Wenli Yang

*Eric Vermote, Science Team Member
University of Maryland*

RAYTHEON SYSTEMS COMPANY
Information Technology and Scientific Services
4400 Forbes Boulevard
Lanham, MD 20706

SBRS Document #: Y2388

NPOESS COMPETITION SENSITIVE

EDRs: AEROSOL OPTICAL THICKNESS AND
PARTICLE SIZE PARAMETER

Doc No: Y2388

Version: 3

Revision: 0

	Function	Name	Signature	Date
Prepared By	Principle Author	H. KILCOYNE		
Approved By	Relevant IPT Lead	H.KILCOYNE		
Approved By	Chief Scientist	P. ARDANUY		
Released By	Program Manager	H. BLOOM		

TABLE OF CONTENTS

	<u>Page</u>
LIST OF FIGURES	v
LIST OF TABLES	vii
GLOSSARY OF ACRONYMS	viii
ABSTRACT	ix
1.0 INTRODUCTION	1
1.1 PURPOSE	1
1.2 SCOPE	1
1.3 VIIRS DOCUMENTS	2
1.4 REVISIONS	2
2.0 EXPERIMENT OVERVIEW	3
2.1 OBJECTIVES OF VIIRS AEROSOL OPTICAL THICKNESS AND SIZE PARAMETER RETRIEVALS	3
2.2 INSTRUMENT CHARACTERISTICS	4
2.3 AEROSOL RETRIEVAL STRATEGIES	4
2.3.1 Aerosol Optical Thickness Retrievals Over Water	4
2.3.2 Aerosol Optical Thickness Retrievals Over Land	5
2.3.3 Aerosol Size Parameter Retrievals	5
3.0 ALGORITHM DESCRIPTION	6
3.1 PROCESSING OUTLINE	6
3.2 ALGORITHM INPUT	8
3.2.1 VIIRS Data	8
3.2.1.1 Cloud Information	8
3.2.1.2 Land/Water Information	8
3.2.1.3 Sun Glint Information	8
3.2.1.3 Snow/Ice Information	9
3.2.1.4 Calibrated TOA Reflectances and Brightness Temperatures	9
3.2.2 Non-VIIRS Data	9
3.2.2.1 Ozone Information	9
3.2.2.2 Total Precipitable Water	9
3.2.2.3 Wind Velocity	10
3.2.2.4 Surface Pressure	10
3.2.2.5 Aerosol Index	10
3.2.2.6 Digital Elevation Model	10
3.2.2.7 Aerosol Climatology	10

3.3	THEORETICAL DESCRIPTION OF AEROSOL OPTICAL THICKNESS AND SIZE PARAMETER RETRIEVALS	11
3.3.1	Read Input Data.....	11
3.3.1.1	Physics of the Problem.....	11
3.3.1.2	Mathematical Description of the Algorithm.....	12
3.3.2	Correction of the Input Reflectances	12
3.3.2.1	Physics of the Problem	12
3.3.2.2	Mathematical Description of the Algorithm.....	12
3.3.3	Snow/Ice Pixel Determination.....	13
3.3.3.1	Physics of the Problem	13
3.3.4	Dark Pixel Determination (Land Only).....	13
3.3.4.1	Physics of the Problem	13
3.3.4.2	Mathematical Description of the Algorithm.....	14
3.3.5	Choose Aerosol Model	14
3.3.5.1	Physics of the Problem	14
3.3.5.2	Mathematical Description of the Algorithm.....	15
3.3.6	Inversion using Look-Up Tables	15
3.3.6.1	Physics of the Problem	15
3.3.6.2	Mathematical Description of the Algorithm.....	16
3.3.7	Calculation of Size Parameter	16
3.3.7.1	Physics of the Problem	16
3.3.7.2	Mathematical Description of the Algorithm.....	16
3.3.8	EDR Requirements	19
3.3.6.1	Error Budget	21
3.4	ALGORITHM SENSITIVITY STUDIES	21
3.4.1	Description of Simulations	21
3.4.2	Calibration Errors	27
3.4.3	Instrument Noise	28
3.4.4	Band Selection.....	30
3.4.5	Other	31
3.5	PRACTICAL CONSIDERATIONS	34
3.5.1	Numerical Computation Considerations	34
3.5.2	Programming and Procedural Considerations	34
3.5.3	Configuration of Retrievals	34
3.5.4	Quality Assessment and Diagnostics.....	34
3.5.5	Exception Handling	34
3.6	ALGORITHM VALIDATION	35
3.6.1	Pre-Launch Validation Studies.....	35
3.6.2	Post-Launch Routine Ground-Based Observations.....	41
3.6.3	Post-Launch Special Field Experiments.....	42
3.6.4	Post-Launch Satellite-Based Intercomparisons.....	42

3.7	ALGORITHM DEVELOPMENT SCHEDULE.....	42
4.0	ASSUMPTIONS AND LIMITATIONS.....	43
4.1	ASSUMPTIONS	43
4.2	LIMITATIONS	43
5.0	REFERENCES.....	44

LIST OF FIGURES

	<u>Page</u>
Figure 1a. Aerosol Module processing outline.	6
Figure 1b. Aerosol Optical Thickness processing outline.....	7
Figure 1c. Aerosol Particle Size Parameter processing outline.	7
Figure 2 Scatter diagram between the surface reflectance 0.49 μm (full symbols) and 0.66 μm (empty symbols) to that at 2.2 μm , for several surface types. The average relationships $\rho_{0.49}/\rho_{2.2}=0.25$ and $\rho_{0.66}/\rho_{2.2}=0.5$ are also plotted (solid lines) (Kaufman and Tanré, 1996).....	14
Figure 3. Size distribution (averaged) observed over two AeRoNet sites. Bahrain (desertic aerosol) and Cuiaba (Biomass burning aerosol).	17
Figure 4. Effective radius approximation using the Ångström exponent calculated from the 670nm and 870nm AeRoNet data.....	18
Figure 5. Effective radius approximation using the Ångström exponent calculated from the 870nm and 1020nm AeRoNet data.....	19
Figure 6: Effective radius approximation using the Ångström exponent calculated from the 633nm and 870nm from 6S simulation using the averaged size distributions derived from AeRoNet.....	22
Figure 7: Effective radius approximation using the Ångström exponent calculated from the 870nm and 1536nm from 6S simulation using the averaged size distributions derived from AeRoNet.....	22
Figure 8. Example of optical thickness retrieval on 1:30 PM orbit over ocean.	23
Figure 9. Example of size parameter retrieval on 1:30 PM orbit over ocean.....	23
Figure 10a. The 3.75 μm channel reflectances of the Chesapeake Bay scene.....	24
Figure 10b. Retrieval results of Chesapeake Bay scene. Figure clearly shows pixels where the aerosol optical thickness of 0.5 was retrieved.....	24
Figure 11a. TERCAT scene of the Olympic Peninsula provided by the IPO. This simulation is on the top subscene.....	25
Figure 11b. The “true” simulated optical thickness.	26
Figure 11c. Optical Thickness Retrieval at 600 m GIFOV.....	26

Figure 11d. Optical Thickness Retrieval at 10.2 km Horizontal Cell Size. Note: Most errors arise from the artificial aerosol optical thickness boundaries produced in the synthetic simulation.	27
Figure 12. Comparison of retrieved optical depth using AVHRR data and the dark target approach with measured optical depth from AERONET in August 1993 over the Eastern United States.	35
Figure 13. Comparison of retrieved optical depth using AVHRR data and the dark target approach with measured optical depth from AERONET in 1993 over Brazil.	36
Figure 14. Empirical relation between the red (0.67 μm) and mid-infrared (3.75 μm) reflectances derived from AVHRR data for November 1997.....	37
Figure 15. Aerosol optical thickness at 0.67 μm for 27-Sept.-97 derived from AVHRR (upper image) and SeaWiFS (lower image) data.	38
Figure 16. Aerosol optical thickness derived from SeaWiFS data for 27-Sept.-97 at 0.443 μm (upper image) and 0.67 μm (lower image).....	39
Figure 17. Retrieval of Aerosol Optical Thickness and Ångström Exponent using SeaWiFS data.....	40

LIST OF TABLES

	<u>Page</u>
Table 1. Summary of Aerosol Optical Thickness and Particle Size Parameter Product	1
Table 2. Ancillary Data from VIIRS Products.....	8
Table 3. Ancillary Data from Other NPOESS Instruments	9
Table 4. Aerosol Optical Thickness.....	19
Table 5. Aerosol Size Parameter.....	20
Table 6. Aggregated Optical Thickness Retrieval Results for Olympic Peninsula Scene at HCS	27
Table 7. Calibration Requirements for Typical Global Mean Aerosol Optical Depth of 0.20.....	28
Table 8. AOT and APS Performances using SBRS Predicted Sensor Model	29
Table 9. Ancillary Data Required by the Optical Thickness and Size Parameter Algorithm.....	32
Table 10. Ancillary Data Required by the Optical Thickness and Size Parameter Algorithm for a Single Pixel	32
Table 11. Calculations of the effect of Pixel Reflectance Differences on Ångström Exponent	33

GLOSSARY OF ACRONYMS

6S	Second Simulation of the Satellite Signal in the Solar Spectrum
AERONET	Aerosol Robotic Network
AOT	Aerosol Optical Thickness
ATBD	Algorithm Theoretical Basis Document
AVHRR	Advanced Very High Resolution Radiometer
CMIS	Conical Scanning Microwave Imager/Scanner
DAO	Data Assimilation Office
DEM	Digital Evaluation Model
EDR	Environmental Data Record
EVI	Enhanced Vegetation Index
FOV	Field of View
GACP	Global Aerosol Climatology Program
IPO	Integrated Program Office
IPT	Integrated Product Team
IR	Infrared
ITSS	Information Technology and Scientific Services (Raytheon)
LUT	Look-up Table
MAS	MODIS Airborne Simulator
MODIS	Moderate Resolution Imaging Spectroradiometer
MODTRAN	Moderate Resolution Transmission Model
NPOESS	National Polar-orbiting Operational Environmental Satellite System
OMPS	Ozone Mapping Profiling Suite
QA	Quality Assurance
SBRS	Santa Barbara Remote Sensing
SeaWiFS	Sea-viewing, Wide Field-of-view Sensor
SNR	Signal-to-Noise Ratio
SRD	Sensor Requirements Document
TOA	Top of the Atmosphere
TOMS	Total Ozone Mapping Spectrometer
VIIRS	Visible/Infrared Imager/Radiometer Suite

ABSTRACT

Atmospheric aerosol plays a role in the Earth's radiation budget through radiative forcing and chemical perturbations. Quantifying this forcing requires accurate information on the global distribution of aerosol optical thickness, size distribution, and single scattering albedo. Aerosols play an important role in global warming by affecting the rate at which warming occurs, as the aerosols effectively cool the atmosphere by influencing the reflective and absorbing properties of clouds. Aerosol information is also vital to the atmospheric correction for the Sea Surface Temperature and Vegetation Index, climate modeling, and battlefield visibility modeling. Due to the high spatial and temporal variability of the aerosol particles, the satellite approach is the only feasible choice. This document describes the operational retrieval algorithm of the Visible/Infrared Imager/Radiometer Suite (VIIRS) aerosol optical thickness and particle size parameter products. Retrieval of these products will be performed globally on a daily basis except over bright surfaces and cloudy conditions. Because the reflective properties of ocean and land are very different, separate retrieval approaches are used over the land and the ocean. Aerosol products are calculated over the ocean using the known reflectance of the ocean surface with look-up tables of pre-computed values of TOA reflectance for several aerosol types, optical thicknesses, and solar and viewing angles. The look-up table accounts for multiple scattering in the atmosphere by molecules and aerosol particles, and angular reflection of the surface. Over the land, a dark pixel method introduced by Kaufman *et al.* (1997) for the Moderate Resolution Imaging Spectroradiometer (MODIS) is adopted to identify areas where dense vegetation allows retrieval. The VIIRS sensor design includes a band at 2.25 μm to detect the dark pixels required for retrieval of optical thickness, and thus aerosol particle size parameter, over land. Measured radiance at satellite level is inverted into the aerosol optical thickness using look-up tables. Error analyses and validations have been performed and the results are presented in this document.

1.0 INTRODUCTION

It is well known that atmospheric aerosol plays an important role in the Earth's radiative budget (Charlson *et al.*, 1992) and affects the global climate through radiative forcing and chemical perturbations. It is also related to the cloud albedo effect through microphysical interactions with cloud particles. Aerosol information is critical for atmospheric correction algorithms and military operations. The climate effects of atmospheric aerosols may be comparable to CO₂ greenhouse effects, but with opposite sign and larger uncertainty (Hansen and Lacis, 1990; IPCC, 1994). To quantify the aerosol radiative forcing, which will be used by the atmosphere correction for the land products, and narrow down its uncertainty, information about global distributions of aerosol optical thickness (AOT) and size distribution is necessary. Due to the high spatial and temporal variability of the aerosol particles, only the satellite approach is feasible for this objective.

1.1 PURPOSE

This Algorithm Theoretical Basis Document (ATBD) describes the algorithm used to retrieve the Aerosol Optical Thickness and Particle Size Parameter Environmental Data Records (EDR) for the Visible/Infrared Imager/Radiometer Suite (VIIRS) instrument on the National Polar-orbiting Operational Environmental Satellite System (NPOESS). These products are summarized in Table 1. Specifically, this document identifies the sources of input data, both VIIRS and non-VIIRS, required for retrieval; provides the physical theory and mathematical background underlying the use of this information in the retrievals; includes implementation details; and describes assumptions and limitations of the proposed approach.

Table 1. Summary of Aerosol Optical Thickness and Particle Size Parameter Product

Parameter Name	Units	Horizontal Cell Size	Comments
Aerosol Optical Depth	Dimensionless	1.6 km (Ocean) 9.6 km (Land)	Retrieved globally except areas of clouds and bright surfaces Reported at several wavelengths between 0.4 and 4.0 μm
Aerosol Particle Size Parameter	Ångström Wavelength Exponent: Dimensionless Effective Radius: μm	1.6 km (Ocean) 9.6 km (Land)	Threshold: Ångström Wavelength Exponent, uses optical depth at pairs of wavelengths Objective: Effective radius determination

1.2 SCOPE

This document covers the algorithm theoretical basis for the retrieval of the aerosol optical thickness and size distribution products of VIIRS on NPOESS. The VIIRS aerosol solution was developed using the MODIS and AVHRR aerosol algorithm heritages.

Section 1 describes the purpose and scope of this document. Section 2 is an overview of the aerosol retrievals. The theoretical description and implementation of the algorithm are described

in Section 3, and the assumptions and limitations of the approach are summarized in Section 4. References for citations in the text are listed in Section 5.

1.3 VIIRS DOCUMENTS

Reference to VIIRS project or reference documents is indicated by a number in italicized brackets, e.g., [Y-1].

[Y-1] Visible/Infrared Imager/Radiometer Suite (VIIRS) Sensor Requirements Document (SRD) for National Polar-orbiting Operational Environmental Satellite System (NPOESS) Spacecraft and Sensors.

[Y-2] NEDL/NEDT Sensor Requirements Flowdown Memo, Aerosol Optical Thickness and Size Parameter, document number RAD.NEDL.AOT.

[Y-2390] VIIRS Suspended Matter Algorithm Theoretical Basis Document.

1.4 REVISIONS

This is the third version of this document dated May 2000; the first version was dated October 1998, and the second version was dated June 1999. The revisions to this document include updates due to algorithm development and insertion of more simulation results.

2.0 EXPERIMENT OVERVIEW

2.1 OBJECTIVES OF VIIRS AEROSOL OPTICAL THICKNESS AND SIZE PARAMETER RETRIEVALS

The objective of this algorithm is to calculate the aerosol optical thickness, proportional to the total aerosol loading of the ambient aerosol, over both land and ocean globally on a daily basis. Because the reflective properties of the Earth's surface under an aerosol layer vary significantly from land type to land type, different methods are used over the land and the ocean. As clouds block the surface reflectance, the aerosol optical thickness cannot be found for cloudy pixels. Retrievals are only performed during the daytime due to the lack of light in the visible channels during the nighttime.

The overall objectives of the VIIRS aerosol retrievals are:

- 1) To determine the aerosol optical thickness, which is an indicator of the amount of direct aerosol radiative forcing on the climate, an input to radiative transfer models used to calculate this forcing, a critical military operations planning tool, and a required input to atmospheric correction algorithms. The aerosol optical thickness is defined in the VIIRS SRD [Y-1] as the “extinction (scattering + absorption) vertical optical thickness of aerosols at multiple wavelengths within the 0.4 – 2.4 μm spectral range based on narrow band (bandwidth < 0.05 μm) measurements. Optical thickness (τ) is related to transmission (t) by $t = \exp(-\tau)$.”
- 2) To determine the aerosol particle size parameter, which is an indicator of the importance of the aerosol effect on radiation. The larger the aerosol, the more important the effect on radiation. Radiatively important sizes range from 0.1 to 10.0 microns. Larger sizes are difficult to determine with current space-based remote sensing measurements. More detailed size distribution information enables a more complete determination of the radiative properties of the aerosols. Aerosols have an indirect radiative forcing through their modification of cloud properties. These effects can be monitored through their changes in size distribution in the vicinity of cloud fields. The threshold size parameter is the Ångström wavelength exponent α (α):

$$\alpha = -\frac{\ln \tau_1 - \ln \tau_2}{\ln \lambda_1 - \ln \lambda_2} \quad (1)$$

To determine the Ångström wavelength exponent, optical thickness in two different narrow wavelength bands separated by at least 200 nm is required. If aerosol particle size distribution is given by an inverse power law, such as a Junge distribution, then α (α) can be related to the exponent in the power law.

The objective size parameter requirement is their effective radius, which is defined as the area weighted average radius of the aerosol particle size distribution. The effective radius provides another approximate measure of the size of the aerosol.

Optical thickness and size parameter retrievals apply only under clear and daytime conditions.

2.2 INSTRUMENT CHARACTERISTICS

The narrow band measurements of the VIIRS sensor in the 0.4 to 4.0 μm range are used to derive aerosol optical thickness. The visible and near infrared channels used to derive optical thickness are all within window regions and their bandwidths are narrow. As a result, the contamination of gas (such as O_2 , O_3 , H_2O) absorption is minimized in direct measurements. For the retrieval over land, mid-IR channels (2.25 and 3.7 μm) are correlated to blue and red channels (0.488 and 0.672 μm) for identification of dark pixels for the retrieval.

2.3 AEROSOL RETRIEVAL STRATEGIES

It has been demonstrated that aerosol optical thickness can be retrieved from solar-reflected radiance, and that aerosol size distribution information is carried in the spectral dependence of aerosol optical thickness (e.g., King *et al.*, 1978; Tanré *et al.*, 1992). Thus, satellite reflectance measurement limited to one (GOES) or two channels (Advanced Very High Resolution Radiometer [AVHRR]) were used first to derive the total aerosol content by assuming a given aerosol model. Then, iterative methods were introduced by Kaufman (1990) and Ferrare (1990) to retrieve more aerosol parameters simultaneously, such as size, single-scattering albedo, and optical thickness. As pointed out by Tanré *et al.* (1996), the success of these methods was limited by their poor accuracy related to limited spectral resolution, inaccurate calibration, and gas absorption contamination. Currently, multiple-channel measurements (e.g., the Moderate Resolution Imaging Spectroradiometer [MODIS]) are adopted to retrieve aerosol parameters. Retrieval accuracy may be improved significantly by selecting channels carefully (to reduce gas or surface contamination) and by introducing correction schemes based on multiple-channel information.

Here, an approach similar to MODIS but more operationally oriented is proposed for VIIRS on NPOESS. Solar-reflected spectral reflectances measured by satellite in well-selected multiple channels of visible and near-IR will be used to derive the aerosol optical thickness and size distribution simultaneously over land and ocean. The core of the approach is to use a look-up table (LUT), which is pre-computed for several values of the aerosol and surface parameters by using sophisticated radiation transfer models (such as Second Simulation of the Satellite Signal in the Solar Spectrum [6S]). The measured spectral reflectances (after pre-processing) are compared with the LUT reflectances to identify the best solution.

2.3.1 Aerosol Optical Thickness Retrievals Over Water

The relatively homogeneous surface of the ocean enables the direct application of the LUT approach to find the aerosol optical thickness and size distribution. Using the observed reflectance at the top of the atmosphere (TOA) in coordination with ancillary information on the wind speed, water vapor, surface pressure, surface elevation, and ozone, the corrected reflectances are inverted into a maritime LUT to find a preliminary value of optical thickness. This value is used to determine a preliminary value of the size parameter and to determine the suspended matter present in the cell. The suspended matter information is then used to choose a better aerosol model, which is used to calculate more accurate values of optical thickness and the size parameter.

2.3.2 Aerosol Optical Thickness Retrievals Over Land

The approach over land is more complicated, in that dark, vegetated surfaces are required for aerosol optical depth retrieval. A near-IR band is used to identify dark, vegetated pixels, then the surface reflectance in the visible bands is calculated from the observed reflectance in the near-IR band. The optical thickness is initially calculated assuming a continental aerosol model, and then a preliminary size parameter and suspended matter are determined. The suspended matter information is used to choose a better aerosol model and more accurate values of optical thickness and size parameter are derived.

We are also investigating the use of backscattered UV radiation to obtain aerosol properties over bright surfaces (such as desert and snow/ice surfaces). It is known that the absorbing characteristics of aerosol particles are more prominent in the UV region than in the visible region. The aerosol scattering effect is strong in the visible region and relatively weak in the UV region. Thus, strong, bright surface reflection can easily contaminate the scattering characteristics of aerosol particles and hide the weak absorbing characteristics in the visible region. However, the stronger absorbing properties displayed in the UV region by absorbing aerosols can be separated from the total signal even over bright surfaces based on the unique absorbing signature displayed through spectral dependence (Torres *et al.*, 1998). This signature has been used successfully by our ozone group at Raytheon ITSS on TOMS data to derive optical properties of absorbing aerosols over bright surfaces (Torres *et al.*, 1998; Hsu *et al.*, 1998). This unique technique, which was developed in our company, may be used in the VIIRS retrieval of absorbing aerosol over bright surfaces, and will be investigated during Phase 2 once OMPS sensor information is made available for use.

2.3.3 Aerosol Size Parameter Retrievals

The Ångström wavelength exponent can be easily calculated from the optical thicknesses in two channels. The SRD definition of the Ångström requires that these bands be separated by at least 200 nm. The band pairs used for the Ångström exponent retrieval will be determined as the algorithm is validated with MODIS data and with help from the OAT. The retrieved Ångström exponent can be related to an effective radius through a relationship derived from observations at 11 AeRoNet sites, and will be determined globally.

3.0 ALGORITHM DESCRIPTION

3.1 PROCESSING OUTLINE

The current processing outline (see Figure 1) is based on the MODIS current operational AVHRR approaches. The VIIRS solution uses the Suspended Matter EDR, which identifies the aerosol type, to choose a more accurate aerosol model. A second calculation of AOT and size parameter is performed using the better aerosol model to improve the aerosol optical thickness and particle size parameter retrievals. The outlines of the Determine AOT and Determine ASP components of the aerosol module are illustrated.

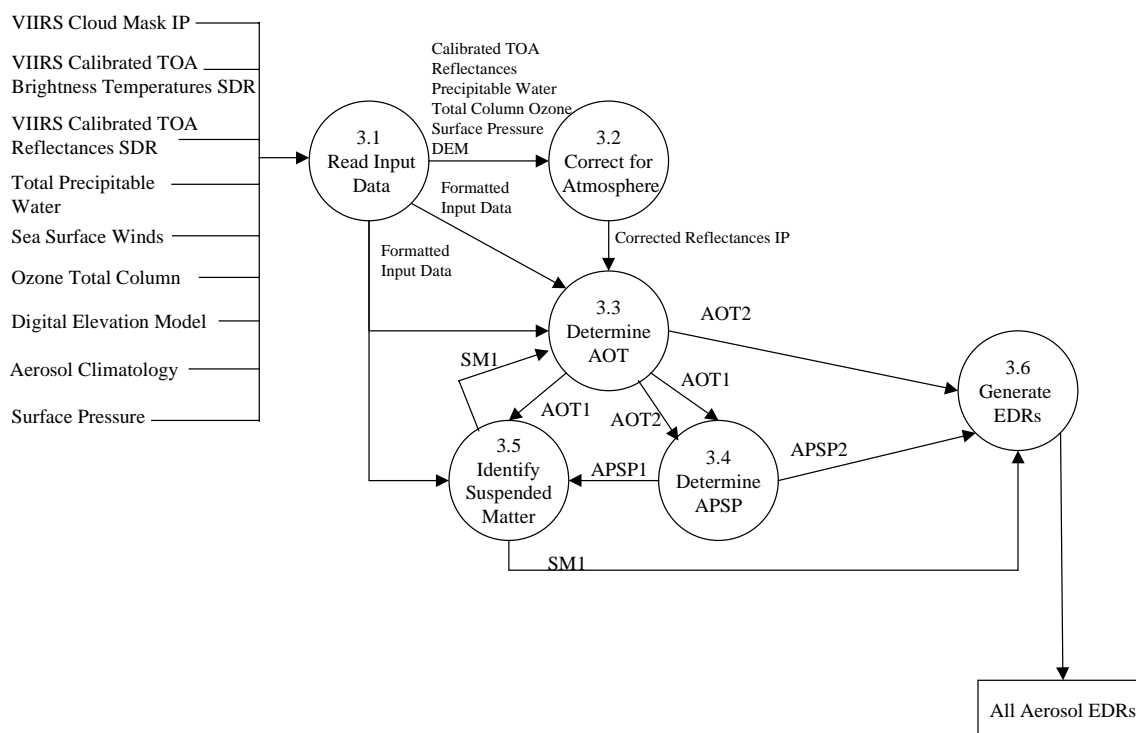


Figure 1a. Aerosol Module processing outline.

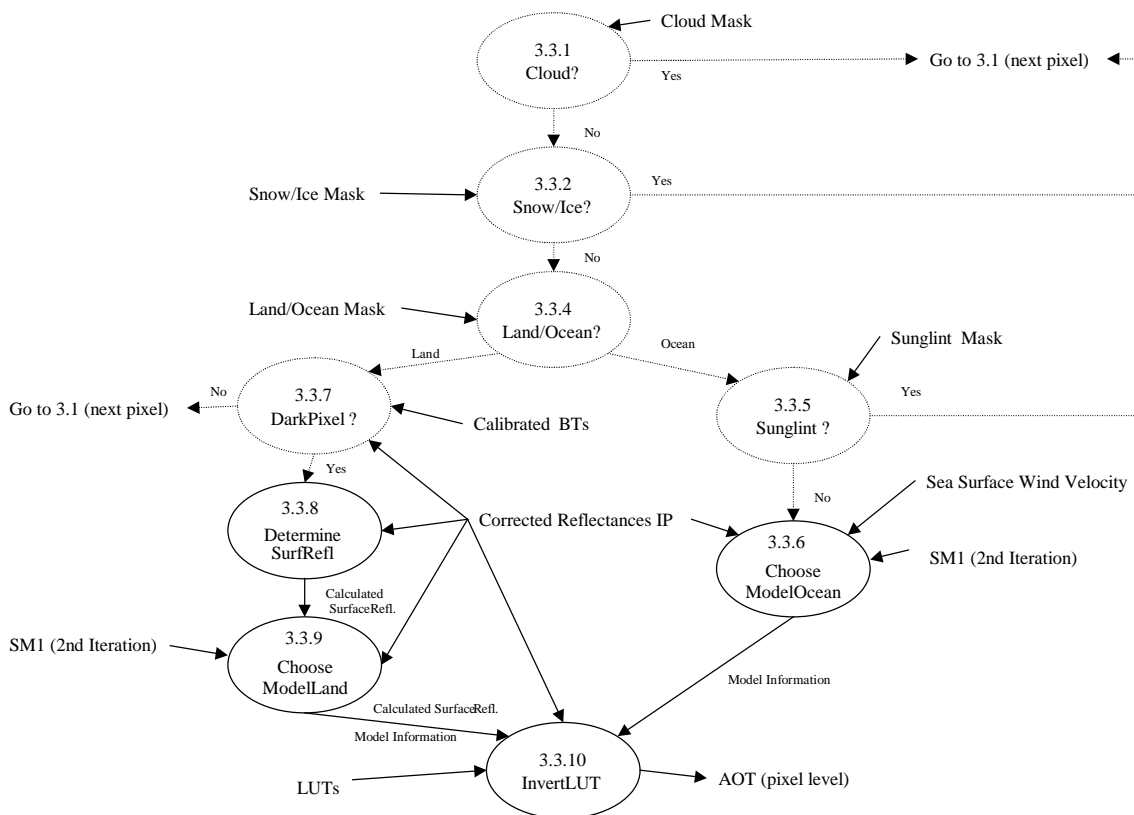


Figure 1b. Aerosol Optical Thickness processing outline.

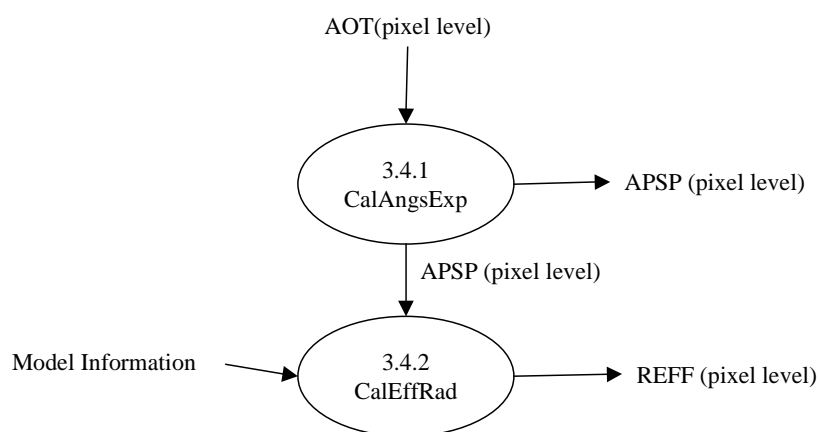


Figure 1c. Aerosol Particle Size Parameter processing outline.

3.2 ALGORITHM INPUT

The algorithm requires ancillary information from the VIIRS instrument and from outside sources. Much of the non-VIIRS data can be obtained from the other instruments on NPOESS. The required accuracies of the ancillary data are currently being examined.

3.2.1 VIIRS Data

The VIIRS data required by the optical thickness and size parameter algorithm are higher-level VIIRS products and are summarized in Table 2 below.

Table 2. Ancillary Data from VIIRS Products

Input Data	Source of Data
Cloud Information	VIIRS Cloud Mask SDR
Land/Water Information	VIIRS Cloud Mask SDR
Sun Glint Information	VIIRS Cloud Mask SDR
Snow/Ice Information	VIIRS Cloud Mask SDR
Calibrated Brightness Temperatures	VIIRS Calibrated TOA Brightness Temperature SDR
Calibrated Reflectances	VIIRS Calibrated TOA Reflectance SDR

3.2.1.1 Cloud Information

The optical thickness and size parameter EDRs are only required for clear or cloud-free conditions; thus, a cloud mask to remove pixels contaminated by cloud cover is needed. A cloud over land will not allow the detection of the dark pixels required for aerosol retrieval, and will cause the optical thickness to be overestimated over the ocean. A quality flag will be included with the Aerosol products to specify areas where clouds may contaminate the retrieval.

3.2.1.2 Land/Water Information

The algorithm for determining optical thickness uses two different procedures depending on whether the pixel is over land or water. Information on the location of the pixel is required. This information will be included in the packet of information received from the cloud mask.

3.2.1.3 Sun Glint Information

The algorithm will not retrieve the optical thickness or size parameter in areas contaminated by sun glint on the ocean surface. Areas of sun glint contamination will be identified by the Cloud Mask, and will be filled in by the next orbit of the next satellite.

3.2.1.3 Snow/Ice Information

Optical thickness in areas of snow and ice cover cannot be retrieved using current algorithms. It is, however, conceivable that further research will lead to a method for its retrieval, in which case the algorithm would be implemented. Areas of snow/ice will be identified by the Cloud Mask.

3.2.1.4 Calibrated TOA Reflectances and Brightness Temperatures

The VIIRS-observed geolocated reflectances and brightness temperatures for some channels are required. These reflectances will be corrected for ozone and water vapor absorption. The solar/viewing angles required for inversion of the corrected reflectances into the aerosol optical thickness LUT will be obtained from these inputs.

3.2.2 Non-VIIRS Data

The source of ancillary data from other NPOESS instruments is given below in Table 3.

Table 3. Ancillary Data from Other NPOESS Instruments

Input Data	Source of Data
Ozone Concentration	NCEP
Total Precipitable Water	NCEP
Wind Velocity	NCEP
Surface Pressure	NCEP
Aerosol Index	OMPS Calibrated Radiance SDR
Digital Elevation Model	VIIRS Calibrated TOA Reflectance SDR
Aerosol Climatology	Database from GACP

3.2.2.1 Ozone Information

The total column amount of ozone is required by the aerosol EDRs to correct the input VIIRS reflectances for absorption by ozone. This data is obtained from the NCEP model data. The threshold horizontal resolution of the ozone EDR is 50 km. This is much larger than the input reflectance resolution of 1 km and the retrieval resolution of 10 km for VIIRS. However, ozone is slowly varying over distance and this discrepancy in resolutions should not be a problem. A backup for the NCEP model data will be the FNMOC(NOGAPS) model data, and then climatology. An accuracy of 15 *milli atm cm* will provide adequate ozone input for the correction.

3.2.2.2 Total Precipitable Water

The total precipitable water amount is required by the aerosol EDRs to correct the input VIIRS reflectances for water vapor absorption. This data will be obtained from the NCEP model data.

As the VIIRS bands were chosen to avoid areas of significant water absorption, the error in the input data should be negligible. FNMOC(NOGAPS) model data will be used as a backup data source.

3.2.2.3 Wind Velocity

The sea surface wind velocity is required for the sun glint and whitecap corrections of the water-leaving radiance used in the calculation of the aerosol optical thickness over the ocean. This information will be supplied by NCEP model data. The wind velocity is used to calculate the Fresnel reflection on the sea surface using the Cox and Munk (1954) rough ocean model. This gives the probability distribution of surface slopes as a function of wind speed and direction. The percentage of the sea covered by sea foam depends on wind speed following Koepke's model (1984). This foam affects the reflectance of the ocean, and this effect is assumed to be independent of wavelength. The resulting effect on optical thickness, size distribution, and effective radius is not large; therefore, the inclusion of the whitecap correction is not vital. The use of the wind velocity in the sun glint correction is also not vital, as the pixels affected by sun glint can alternately be removed by not considering pixels within $\pm 30^\circ$ of the solar zenith and azimuth angles. FNMOC(NOGAPS) model data will be used as a backup data sources. A constant wind velocity can be assumed as another alternative.

3.2.2.4 Surface Pressure

The surface pressure is used to calculate the Rayleigh, or molecular, scattering correction of the input VIIRS reflectances. The surface pressure will be obtained from the NCEP model data. As a backup data source, FNMOC(NOGAPS) model data will be used.

3.2.2.5 Aerosol Index

Absorption is one of the largest uncertainties in the retrieval of aerosol optical thickness and size parameter. An absorbing index produced from the 340 and 380 nm channels of OMPS on NPOESS can be used to help differentiate suspended matter and minimize the errors associated with this retrieval. This product may also aid in determining the vertical distribution of suspended matter. The radiances as measured by OMPS are the only data required for this index.

3.2.2.6 Digital Elevation Model

A digital elevation model is required to calculate the exact surface pressure for a particular location. We will use the ETOPO5 DEM that is available at a 5 minute resolution.

3.2.2.7 Aerosol Climatology

For atmospheric corrections, an aerosol climatology is needed for those cases where no VIIRS aerosol optical thickness measurements exist. Initially, the preliminary aerosol climatology of the Global Aerosol Climatology Program (GACP) will be used (Geogdzhayev and Mishchenko, 1999). This climatology has a 1 by 1 degree spatial resolution and gives monthly means. It is based on NOAA-9 observations and gives the aerosol optical depth and size distribution over oceans. The GACP climatology is not fully satisfactory for our purposes since it does not provide

values over land. It is anticipated that improved GACP aerosol climatologies will become available using MODIS, MISR, SeaWiFS, and other sensors. These will be available before the first launch of VIIRS. Eventually, we expect VIIRS itself to generate an aerosol climatology that will be used for VIIRS.

3.3 THEORETICAL DESCRIPTION OF AEROSOL OPTICAL THICKNESS AND SIZE PARAMETER RETRIEVALS

Over both land and ocean, the signal received by the satellite is a combination of contributions from two sources: the atmospheric radiative transfer process and the surface reflectance. The surface reflectance differs significantly depending on surface type. Over the ocean, the surface is relatively homogeneous and the surface reflectance relatively constant. A look-up table accounting for multiple scattering in the atmosphere by molecules and aerosol particles and angular reflection of the surface can be used along with the known reflectance of the ocean surface to calculate the aerosol optical depth. The water-leaving radiance is dependent upon the chlorophyll content, or ocean color, and the turbidity. In rough seas, sea foam and whitecaps can alter the water-leaving radiance; therefore, the spectral reflection of rough seas is calculated using the Cox and Munk (1954) model. In this model, the wind speed is needed to estimate sea foam. This correction may not be necessary to meet the VIIRS requirements. Sun glint is a source of error in the algorithm, as it can cause the water surface to be bright. Therefore, in areas of sun glint, the optical thickness is not calculated. Sun glint regions can be eliminated using viewing and illumination geometries.

Over the land, the surface albedo varies with wavelength. Areas of dark, dense vegetation have a very low reflectance in the red and blue regions. Aerosols will make these regions appear brighter as they scatter the light as it travels back to the sensor from the surface. In the middle IR, the wavelength of the radiation is too long to be affected by this scattering and thus provides a more accurate representation of the surface. Previous work by Kaufman *et al.* (1997) for MODIS has established a relationship between the reflectances in the middle IR and in the red and blue regions. This statistical relationship is used to calculate surface reflectance in the visible range from the measured reflectance in the middle IR. A process of elimination finds regions dark enough for this application to work. A pixel must meet a series of criteria, including a low enough reflectance and a certain brightness temperature, in order to be considered dark, thus preventing bright pixel (e.g., snow and sand) selection.

3.3.1 Read Input Data

3.3.1.1 Physics of the Problem

The aerosol module uses data from VIIRS, other NPOESS instruments, and data from outside sources. The Read Input Module reads in the ancillary/auxiliary data that has been pre-processed by the SDR module and readies it for use by the following components of the aerosol module. The data not directly used by the module for optical depth, size parameter, or suspended matter calculation, is used for quality checks of the products, such as identification of cloud or sunglint contamination. The aerosol retrievals are only required for non-cloudy daytime conditions. Therefore, any data contaminated by cloud cover not within the daytime definition will be flagged. The definition of “daytime” for the aerosol EDRs has been established to be solar

zenith angles less than 70°, and “cloudy” has been defined as any cloud cover within a pixel. The VIIRS Cloud Mask SDR will provide information on cloud cover, land type, snow/ice contamination, and sun glint contamination. The algorithm will use this information to determine which optical thickness retrieval method is used since land and ocean each have different methods of retrieval.

3.3.1.2 Mathematical Description of the Algorithm

The cloud mask information for each pixel is read. Currently, the cloud mask information will be provided in three bytes. The first byte contains the information required by the optical thickness algorithm for retrieval of optical thickness. The first bit indicates the quality of the cloud mask information as okay (1) or questionable (0). The second two bits are the actual cloud flag and label the pixel as “cloudy” (11), “probably cloudy” (10), “confident clear” (01), and “clear” (00). If the pixel is considered “cloudy” by the cloud mask, the pixel will be discarded and the algorithm will move to the next pixel. The fourth bit provides the sun glint information, as either “glint” (1) or “no glint” (0). The fifth bit provides the snow/ice cover information, labeling the pixel as either containing snow/ice (1) or not (0). The last three bits of the first byte of information provide the land/water surface information. The pixel is labeled either “land” (111), “water” (000), “coastal” (010), or “desert” (011). The non-cloud mask information is read and stored for later algorithm action.

3.3.2 Correction of the Input Reflectances

3.3.2.1 Physics of the Problem

Some of the VIIRS bands are located in regions of absorption by water vapor and ozone. In order to account for this absorption so that they do not influence the optical thickness retrieval, the observed reflectances must be corrected for absorption by these gases using ancillary data information from other NPOESS instruments. Molecular, or Rayleigh, scattering, must also be calculated and the reflectances corrected to account for this scattering.

3.3.2.2 Mathematical Description of the Algorithm

To account for absorption by atmospheric gases, the reflectance at the top of the atmosphere, $\rho_{TOA}(\mu_s, \mu_v, \phi)$, is modified:

$$\rho_{TOA}(\theta_s, \theta_v, \phi_s - \phi_v) = T_g(O_3, M) \left\{ \rho_r + (\rho_0 - \rho_r) T_g^{H_2O}(M, \frac{U_{H_2O}}{2}) + T^\perp(\theta_s) T^\top(\theta_v) \frac{\rho_s}{1 - S \rho_s} T_g^{H_2O}(M, U_{H_2O}) \right\} \quad (2)$$

with ρ_0 the path radiance (in reflectance units), ρ_r the molecular intrinsic reflectance, ρ_s the surface reflectance with no atmosphere above it, and S the reflectance of the atmosphere for isotropic light entering the base of the atmosphere. M is the air mass given by $M = \frac{1}{\mu_s} + \frac{1}{\mu_v}$ and μ_s and μ_v are the cosine of solar and viewer zenith angles. $T_g(O_3, M)$ is the transmittance through the ozone absorption, which is given by $T_g(O_3, M) = \frac{1}{1 + a(M[O_3])^b}$ with $[O_3]$ the ozone column amount (in units of cm/atm), and a and b the coefficients which depend on the response of the given spectral band of ozone. U_{H_2O} is the total precipitable water in units of g/cm². It is assumed

that the path radiance, ρ_0 , is generated above the middle of the boundary layer. Thus, the additional attenuation is caused by half of the precipitable water. The formula adopted for the water vapor transmission is given by $T_s^{H,O}(M, U_{H,O}) = \exp\{-\exp[a + b \ln(MU_{H,O}) + c \ln(MU_{H,O})^2]\}$ with a, b, and c the coefficients, which depend on the response of the given spectral band of water vapor.

3.3.3 Snow/Ice Pixel Determination

3.3.3.1 Physics of the Problem

The cloud mask information on snow/ice cover in the pixel read in the previous step is applied here. If the pixel does contain snow or ice cover, then the optical thickness is not retrieved. If aerosol optical thicknesses are required, then the aerosol climatology information can be used.

3.3.4 Dark Pixel Determination (Land Only)

3.3.4.1 Physics of the Problem

The land type information provided by the cloud mask is applied in this step of the algorithm. If the pixel is considered “land”, then the optical thickness will be retrieved using the method over land. The theory behind remote sensing of aerosol optical thickness over land is based on the approach to be used on MODIS developed by Kaufman *et al.* (1997) on the relationship between the measured reflectance at the top of the atmosphere (ρ^*) and the surface bi-directional reflectance properties $\rho(\theta_v, \theta_s, \phi)$:

$$\rho^*(\theta_v, \theta_s, \phi_s - \phi_v) = \rho_a(\theta_v, \theta_s, \phi_s - \phi_v) + \frac{F_d(\theta_s)T(\theta_v)\rho(\theta_v, \theta_s, \phi_s - \phi_v)}{(1 - s\rho')} \quad (3)$$

$F_d(\theta_s)$ = normalized downward total flux for zero surface reflectance

$T(\theta_v)$ = upward total transmission into the direction of the satellite field of view

$\rho(\theta_v, \theta_s, \phi_s - \phi_v)$ = surface bi-directional reflectance properties

s = atmospheric backscattering ratio

ρ' = surface reflectance averaged over the view and illumination angles

$\rho_a(\theta_v, \theta_s, \phi_s - \phi_v)$ = path radiance

Assuming single scattering, the path radiance is proportional to the aerosol optical thickness (τ_a), the aerosol scattering phase function (P_a), and the single scattering albedo (ω_s).

$$\rho_a(\theta_v, \theta_s, \phi_s - \phi_v) = \rho_{molec}(\theta_v, \theta_s, \phi_s - \phi_v) + \frac{\omega_s \tau_a P_a(\theta_v, \theta_s, \phi_s - \phi_v)}{(4\mu_v \mu_s)} \quad (4)$$

Given the top of the atmosphere radiance, the molecular scattering, and the surface reflectance, an aerosol model can provide the values of ω_s and P_a , which can all be used to determine the aerosol optical depth. Because the aerosol (path) radiance is larger for shorter wavelengths and for low values of the surface reflectance, the errors in deriving the aerosol optical thickness are smaller for these conditions. Therefore, dark, vegetated regions are required for retrieval of aerosol optical thickness over land. Pixels over land must be checked to see if they meet the specified dark pixel criteria. If a pixel is considered dark, then the reflectance in the near-IR

region is used to calculate the reflectance in the visible bands without the influence of aerosol. The relationship between the near-IR and the visible bands must be established for the data set before the algorithm is operational.

3.3.4.2 Mathematical Description of the Algorithm

The reflectance in the 2.1 μm band will be used for the dark pixel determination. The reflectance must fall between specified values to be considered dark. If a pixel is dark, then the retrieval of optical thickness is performed for that pixel; if the pixel fails to meet the criteria, then the retrieval is not performed for that pixel and the algorithm moves on to the next pixel. As the horizontal cell size of the product (9.6 km) is larger than the pixel size (1.6 km), if a cell contains at least one dark pixel within its boundaries, a value for that cell will be reported.

An algorithm developed using AVHRR data was modified to work with VIIRS simulated data on synthetically simulated scenes of the Olympic Peninsula, Bangladesh, and Colombia. The dark pixel criteria for these scenes is relatively simple, the reflectance of the 2.13 μm band must be between 0.0 and 0.09, the reflectance in the 0.85 μm must be between 0.1 and 0.3, and the brightness temperature of the 11.0 μm band must be greater than 289 K. Figure 2 shows the relationships between the surface reflectances for several surface types.

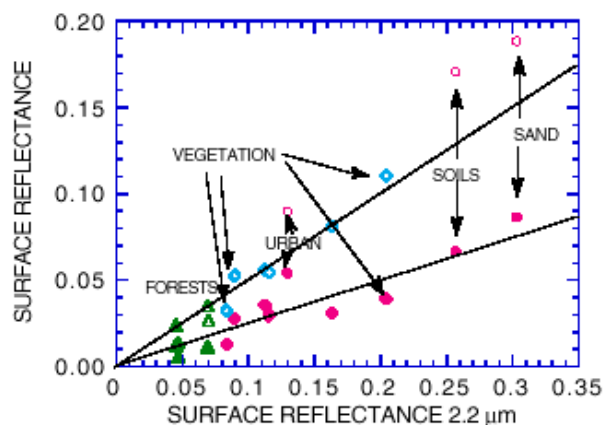


Figure 2. Scatter diagram between the surface reflectance 0.49 μm (full symbols) and 0.66 μm (empty symbols) to that at 2.2 μm , for several surface types. The average relationships $\rho_{0.49}/\rho_{2.2}=0.25$ and $\rho_{0.66}/\rho_{2.2}=0.5$ are also plotted (solid lines) (Kaufman and Tanré, 1996).

3.3.5 Choose Aerosol Model

3.3.5.1 Physics of the Problem

The accuracy of the aerosol optical thickness retrieval is very dependent on the use of the correct aerosol model. The most accurate representation of the aerosol within the pixel must be chosen and the corresponding LUT used. The VIIRS aerosol algorithm uses an iterative method to

assure selection of the most appropriate aerosol model. A preliminary aerosol optical thickness (and subsequent Ångström exponent) are calculated using a continental aerosol model over land surfaces and a maritime aerosol model over ocean surfaces. These preliminary optical thickness and Ångström exponents are used to help determine the type of aerosol present using the Suspended Matter methods described in the VIIRS Suspended Matter ATBD [Y-2390]. The Suspended Matter information retrieved is then used to select a more appropriate aerosol model and a more accurate optical thickness and size parameter are calculated.

3.3.5.2 Mathematical Description of the Algorithm

During the first iteration of the aerosol module, a continental aerosol model over land and a maritime aerosol model over ocean are assumed. The aerosol optical thickness, Ångström exponent, and effective radius are calculated. The Suspended Matter component uses these preliminary retrievals with the VIIRS calibrated reflectances and brightness temperatures [Y-2390] and determines the most probable aerosol type. This aerosol type information is fed back into the aerosol optical thickness component and is used to select a better aerosol model. For example, the suspended matter techniques may determine that smoke is the most probable type of aerosol present within the pixel. The Choose Aerosol Model component of the Aerosol Optical Thickness component would then choose the biomass aerosol model and the accompanying LUT for the inversion of the pixel corrected reflectance to obtain the AOT. The improved AOT is used to calculate an improved Ångström exponent and effective radius.

3.3.6 Inversion using Look-Up Tables

3.3.6.1 Physics of the Problem

Look-up Tables are used to find the aerosol optical properties (optical thickness, phase function, single-scattering albedo, etc.) corresponding to various aerosol models. The tables consist of pre-computed reflectances that would exist at the top of the atmosphere given specific aerosol conditions corresponding to the various aerosol models. The reflectances for 10 optical depths between the required measurement range of 0 to 2.0 are used. The best fit (least squares) between the observed top of the atmosphere reflectance and a pre-computed reflectance determines the aerosol model or optical thickness.

The algorithm will use a variety of aerosol models to provide an accurate determination of the aerosol optical thickness. Over land, the tropospheric aerosol varies with latitude, longitude, and season. The geographic area also influences the type of aerosol present. Urban/industrial aerosols have different properties than rural aerosols. Over the ocean, more LUTs are needed to account for the variety of surface conditions that are possible as wind velocity and sun glint change. Suspended matter information, which is derived using a preliminary determination of AOT and APSP with a series of tests for specific types of suspended matter will be used to determine the most accurate aerosol model and atmospheric model for a particular situation.

3.3.6.2 Mathematical Description of the Algorithm

The LUTs currently being used were generated using the 6S radiative transfer model. Reflectances corresponding to 22 solar zenith angles (2.841 to 81.62 degrees), 22 viewing zenith angles, 73 azimuthal angles between sun and satellite (0 to 180 degrees), and 10 optical thicknesses (0.05 – 2.0) are stored in separate tables for ocean and land. Each band has a different table or set of reflectances. The observed reflectance is then compared to the LUTs and the optical thickness for that pixel derived. The optical thicknesses for all pixels within a horizontal cell are then averaged to give a value for the horizontal cell. The standard deviation, the number of pixels used in the 10km box, and other aerosol quality flags are also calculated and stored.

3.3.7 Calculation of Size Parameter

3.3.7.1 Physics of the Problem

The aerosol size parameter is defined as the Ångström wavelength exponent (α), where:

$$\alpha = -\frac{\ln \tau_1 - \ln \tau_2}{\ln \lambda_1 - \ln \lambda_2} \quad (5)$$

The SRD definition requires that bands 1 and 2 be narrow bands separated by at least 200 nm. If the aerosol particle size distribution is given by an inverse power law, such as a Junge distribution, then alpha can be related to the exponent in the power law.

The effective radius is defined as “the area weighted average radius of the aerosol particle size distribution, or equivalently, the ratio of the third to the second moments of the size distribution” [Y-I].

$$r_{eff} = \frac{\int r^3 \frac{dN(r)}{d \ln(r)} d \ln(r)}{\int r^2 \frac{dN(r)}{d \ln(r)} d \ln(r)} \quad (6)$$

3.3.7.2 Mathematical Description of the Algorithm

The Ångström exponent is calculated directly from the derived optical thicknesses of two bands using Equation 5.

An approximation of the effective radius can be retrieved from a relationship derived from AeRoNet measurements. From AeRoNet data we have access to size distribution ($dV(r)/d \ln(r)$) of aerosol ranging from 0.05 μ m to 15 μ m, so we will compute the effective radius as:

$$r_{eff} = \frac{\int_{r=0.05\mu m}^{r=15\mu m} \frac{dV(r)}{d \ln(r)} d \ln(r)}{\int_{r=0.05\mu m}^{r=15\mu m} \frac{1}{r} \frac{dV(r)}{d \ln(r)} d \ln(r)} \quad (7)$$

Knowing that:

$$\frac{dV(r)}{d \ln(r)} = V(r) \frac{dN(r)}{d \ln(r)} = \frac{4}{3} \pi r^3 \frac{dN(r)}{d \ln(r)} \quad (8)$$

The VIIRS effective radius solution uses a relationship derived between the Ångström exponent and the effective radius. For example on Figure 3, there are two typical size distributions, one observed over Brazil (Cuiaba) and one observed over a desertic site (Bahrain). The Cuiaba effective radius of that distribution is $0.18\mu m$, the effective radius corresponding to the size distribution observed at Bahrain is $0.4\mu m$.

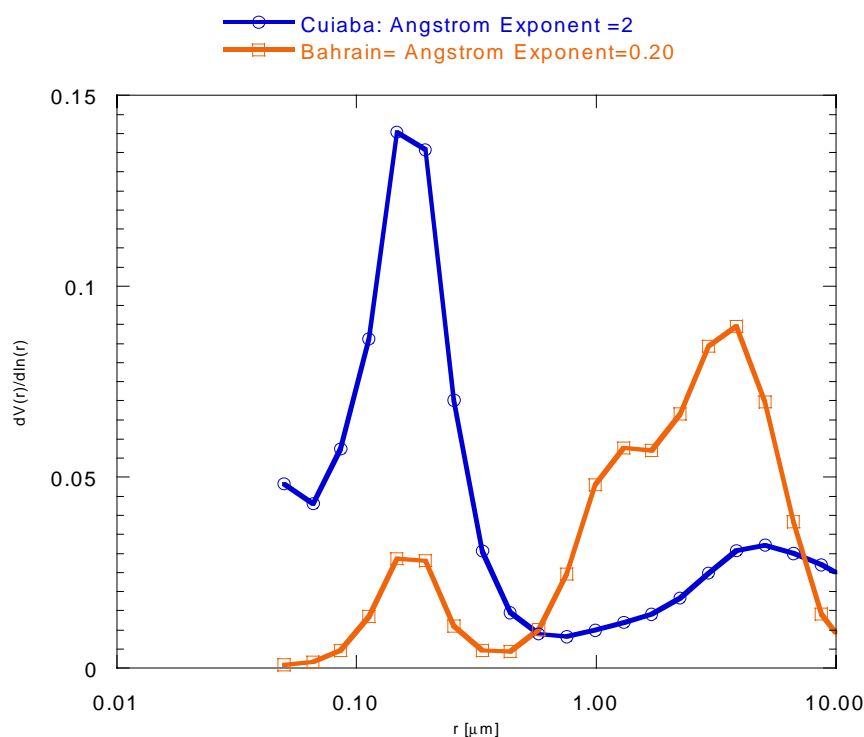


Figure 3. Size distribution (averaged) observed over two AeRoNet sites. Bahrain (desertic aerosol) and Cuiaba (Biomass burning aerosol).

We have compiled statistics for approximately 60 possible sites/instruments of the AeRoNet networks. Size distribution and effective radius are binned by Ångström exponent classes. This is comparable to the procedure used by Kaufman et al. in establishing the aerosol dynamic model (Aerosol ATBD, Kaufman et al., 1998). This model was established to minimize the uncertainty

in the size distribution retrieval while keeping the inherent variability by only averaging by sites (therefore keeping the variability between the different types of aerosols). Several criteria were used to eliminate uncertainties/variations. The number of observations in a given bin had to be greater than a certain threshold (10 obs), the standard deviation of the effective radius within a bin had to be lower than 10%, and the optical thickness at 1020nm had to be greater than 0.15. The results of the study are presented in Figure 4 and 5 and show very clearly that a much better correlation could be established between the Ångström exponent derived from the longer wavelengths available from AeRoNet data (870nm and 1020nm), than from the shorter wavelengths (670nm and 870nm). This may suggest the use of even longer wavelengths on VIIRS such as 865nm and 1600nm will improve the results for bigger particles. Simulations using the 6S code and “actual” averaged size distribution observed by AeRoNet this theory as shown in Figures 6 and 7.

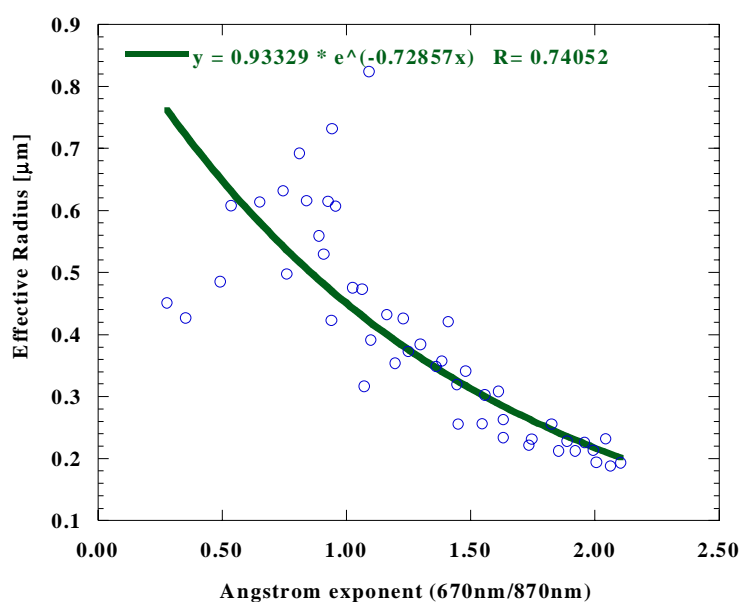


Figure 4. Effective radius approximation using the Ångström exponent calculated from the 670nm and 870nm AeRoNet data

Due to better results obtained from using the Ångström exponent derived from the longer wavelengths for effective radius retrieval, the VIIRS Aerosol Particle Size Parameter will only provide effective radius retrievals over ocean. The effective radius can be retrieved with an accuracy of 17-25% for the Bahrain and Cuiaba sites using the relationship derived between the Ångström exponent and effective radius shown in Figure 5. The Bahrain site has an Ångström exponent of 0.20, which corresponds to an effective radius of 0.5μm. The AeRoNet derived effective radius is 0.4. The effective radius was estimated with an accuracy of 25%. The Cuiaba site has an Ångström exponent of 2.0, which corresponds to an effective radius of 0.21μm using the derived relationship. This retrieval differs from the AeRoNet effective radius retrieval of 0.18 by 17%. Though these accuracy results do not yet achieve the objective requirements as stated by the SRD of 10% over ocean, further development of this procedure using MODIS data

will be possible during Phase 2. The VIIRS effective radius retrieval method is a very simple, operationally oriented solution for the retrieval of this parameter.

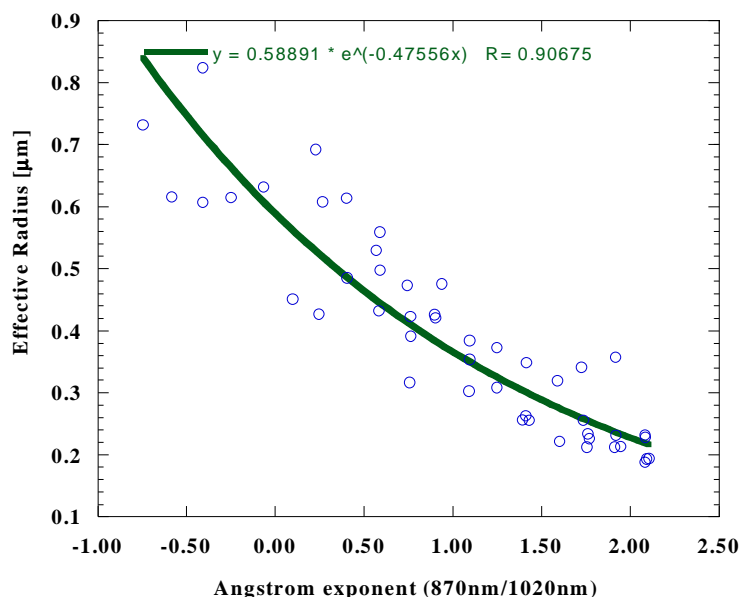


Figure 5. Effective radius approximation using the Ångström exponent calculated from the 870nm and 1020nm AeRoNet data

3.3.8 EDR Requirements

The requirements that must be fulfilled by the algorithm product are defined in the SRD [Y-1] published by the Integrated Program Office (IPO) are listed in Tables 4 and 5. The threshold requirement is the value that must be achieved by the algorithm, and the objective requirement is the value at which the product is desired.

Table 4. Aerosol Optical Thickness

Requirement	Threshold	Objective
Horizontal Cell Size	10 km	1 km
Horizontal Reporting Interval	(TBD)	(TBD)
Vertical Cell Size	30 km (Total Column)	50 km
0 - 2 km	N/A	0.25 km
2 - 5 km	N/A	0.5 km
> 5 km	N/A	1 km
Vertical Reporting Interval	N/A (Total Column)	Vertical Cell Size
Horizontal Coverage	Global	Global
Vertical Coverage	0 – 30 km	0 – 50 km
Measurement Range	0.0 – 2.0	0.0 – 10.0
Measurement Accuracy		
Over Ocean	0.03	0.01
Over Land	0.2	0.1

Table 4. Aerosol Optical Thickness (continued)

Requirement	Threshold	Objective
Measurement Precision		
Over Ocean	0.03	0.01
Over Land	0.20	0.1
Measurement Uncertainty (over Land)	0.05 + 0.2 τ (TBR)	(TBD)
Long-Term Stability	0.01	0.003
Mapping Uncertainty	4 km	1 km
Maximum Local Average Revisit Time	6 hrs (TBR)	4 hrs (TBR)
Maximum Local Refresh	(TBD)	(TBD)
Minimum Swath Width	3000 km (TBR)	(TBR)
Number of Wavelengths	3	8
Wavelength Range	0.4 to 2.4 μm	0.3 to 4.0 μm

Table 5. Aerosol Size Parameter

Requirement	Threshold (Pertaining to Ångström wavelength exponent)	Objective (Pertaining to effective radius)
Horizontal Cell Size	10 km	1 km
Horizontal Reporting Interval	(TBD)	(TBD)
Vertical Cell Size	30 km (Total Column)	
0 - 2 km	N/A	0.25 km
2 - 5 km	N/A	0.5 km
> 5 km	N/A	1 km
Vertical Reporting Interval	N/A (Total Column)	Vertical Cell Size
Horizontal Coverage	Global	Global
Vertical Coverage	0 - 30 km	0 - 50 km
Measurement Range	-1 to +3	0.05 to 5 μm
Measurement Accuracy	0.3 over Ocean 1.0 over Land	10 % over Ocean 30% over Land
Measurement Precision	0.3 over Ocean 1.0 over Land	10 % over Ocean 30% over land
Long-Term Stability	0.1	5 %
Mapping Uncertainty	4 km	1 km
Maximum Local Average Revisit Time	6 hrs (TBR)	4 hrs (TBR)
Maximum Local Refresh	(TBD)	(TBD)
Minimum Swath Width	3000 km (TBR)	(TBD)

3.3.6.1 Error Budget

The accuracy of the algorithm is the combination of all of the errors affecting the product of the algorithm. The major source of errors in the derived aerosol optical thickness and size parameter are uncertainties in the surface reflectance and in the aerosol model used to generate LUTs for retrieval. For ocean surface, the main uncertainties in the surface reflectance are related to contamination by sun glint and whitecaps. To estimate their impact on the optical thickness, we can add errors separately to the reflectance for each channel according to the procedures used by Kaufman *et al.* (1997) for MODIS aerosol retrieval. Over land, the error is mainly due to unexpected surface properties and to contamination by snow, ice, or water. These errors are based on control of the surface reflectance in selecting dark targets. Aerosol model uncertainties primarily affect the LUT values through uncertainties in the aerosol indices of refraction and through the assumption of spherical particles (Mishchenko *et al.*, 1995). These uncertainties may be examined by checking the sensitivity of retrieval products with respect to refractive index (or single scattering albedo) and asymmetry parameter.

Other errors may be introduced indirectly to the final EDR products. These include instrument calibration and stability error, geolocation mapping error, and errors in ancillary data. All the errors are discussed in detail in the “VIIRS Error Budget” document (Y3249).

3.4 ALGORITHM SENSITIVITY STUDIES

3.4.1 Description of Simulations

The algorithm, developed to work with data from AVHRR and the Sea-viewing Wide Field-of-view Sensor (SeaWiFS), has been modified to be tested with VIIRS-like simulations. To analyze the algorithm over the ocean, the algorithm has been applied to a 1:30 PM and a 9:30 AM simulated orbit generated from the viewing angles. See Figures 6 and 7 for examples of retrieval on a 1:30 PM simulated orbit. The reflectances of the orbit were generated using 6S assuming a constant surface reflectance of 0.025 and a marine aerosol. The land algorithm has been analyzed using a simulated scene of the Chesapeake Bay (see Figures 10a and 10b). The algorithm has also been applied to the synthetically simulated scenes of the IPO-supplied TERCAT scenes of Utah’s Great Basin region, the Olympic Peninsula, Bangladesh, and Colombia. The Olympic Peninsula retrieval is shown in Figure 9.

For optical thickness retrieval on the 1:30 PM and 9:30 AM orbits, four optical thicknesses (0.05, 0.15, 0.5, and 2.0) have been chosen in the sensitivity study of accuracy to cover the dynamic region of optical thickness. Results indicate that, for a full swath $[-57.7^\circ, 56.7^\circ]$, objective accuracy (0.01) can be achieved for the first three selected optical thicknesses while only threshold accuracy (0.03) can be achieved for very large optical thicknesses ($\tau=2.0$). One example for $\tau=0.15$ on the 1:30 PM orbit is given in Figure 8. Furthermore, five size parameters ($\alpha=-1, 0, 1, 2, 3$) from a user defined aerosol model have been used in the sensitivity study of accuracy to cover the dynamic region of size parameter for the retrieval on both the 1:30 PM and 9:30 AM orbits. The retrieval algorithm may obtain sufficient accuracy (0.03) between 50° S and 60° N for a full swath as indicated in Figure 9.

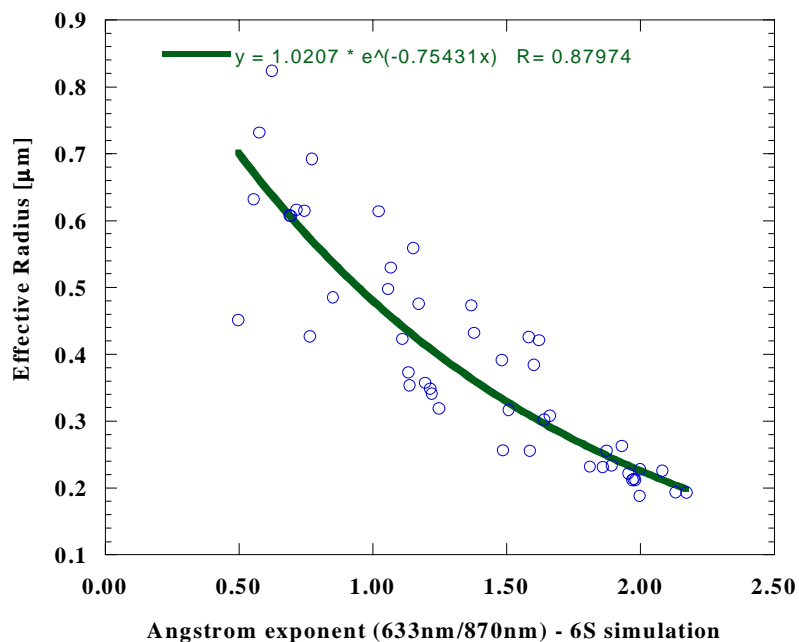


Figure 6: Effective radius approximation using the Ångström exponent calculated from the 633nm and 870nm from 6S simulation using the averaged size distributions derived from AeRoNet.

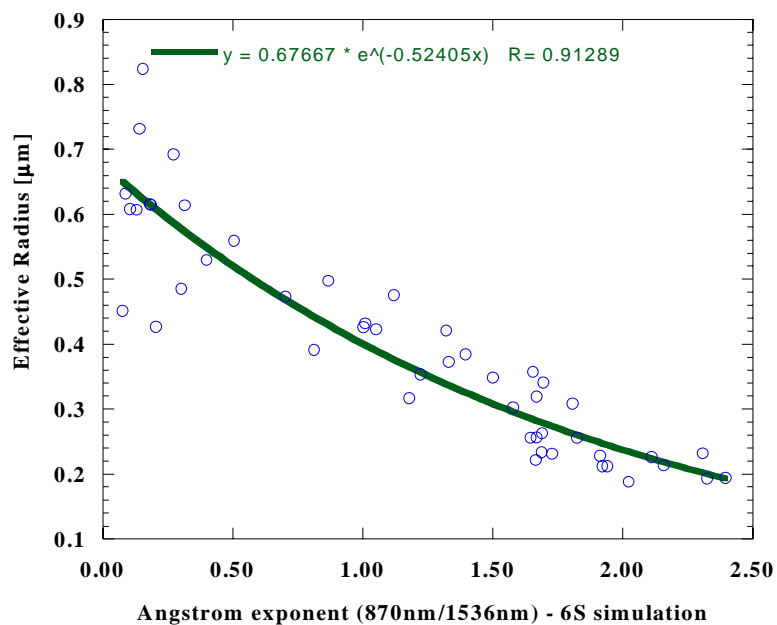


Figure 7: Effective radius approximation using the Ångström exponent calculated from the 870nm and 1536nm from 6S simulation using the averaged size distributions derived from AeRoNet.

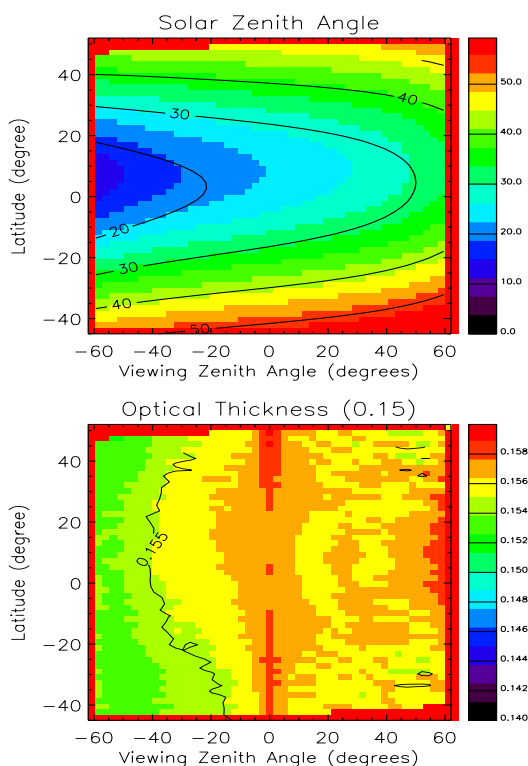


Figure 8. Example of optical thickness retrieval on 1:30 PM orbit over ocean.

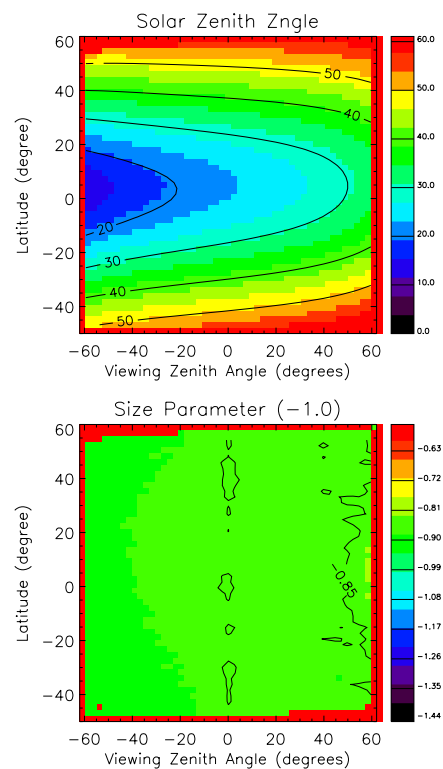


Figure 9. Example of size parameter retrieval on 1:30 PM orbit over ocean.

To verify the retrieval over land, we also applied the retrieval algorithm to simulated scenes of the Chesapeake Bay, the Olympic Peninsula, and Bangladesh generated by Dr. Yang. The Chesapeake scenes were generated using the 6S radiative transfer model with a continental aerosol model. The observation geometry is fixed for every pixel with a solar zenith angle of 25° , view zenith angle of 20° , and the difference between the solar azimuth angle and view azimuth angle of 180° . The resolution of the scenes used for retrieval is about 1×1 km (comparable to the resolution of VIIRS). Fourteen land class types are used along with 5 aerosol optical thicknesses ($\tau=0.05, 0.15, 0.5, 1.0$, and 1.4). A scene of Channel 10 ($\lambda=3.75 \mu\text{m}$) reflectance is presented in Figure 10a as an example. The corresponding optical thickness (with a true value of $\tau=0.5$) retrieved from Channel 5 ($\lambda=0.645 \mu\text{m}$) is displayed in Figure 10b. The accuracy and precision (associated with sensor noise) of the retrieval have also been investigated and are presented in subsection 3.4.3.

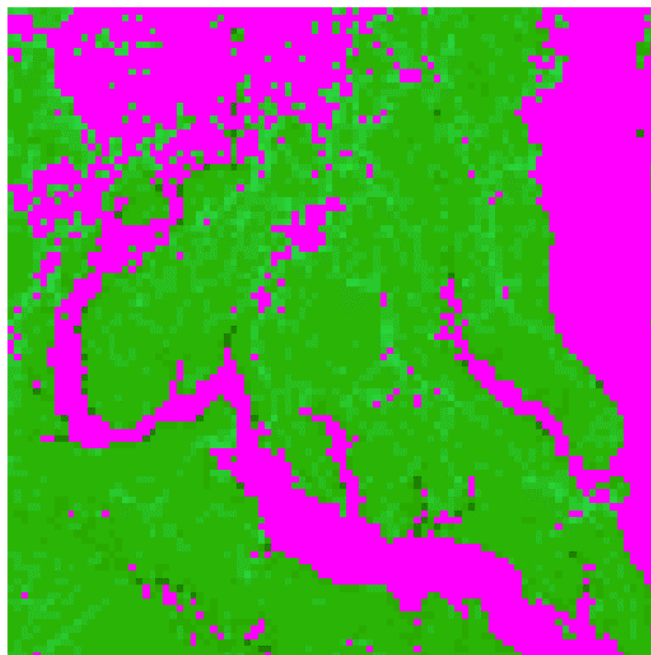


Figure 10a. The 3.75 μm channel reflectances of the Chesapeake Bay scene.

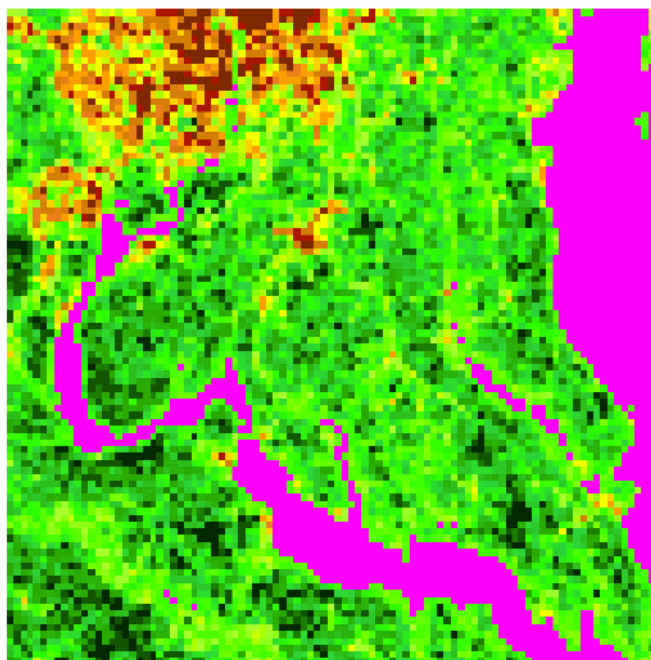


Figure 10b. Retrieval results of Chesapeake Bay scene. Figure clearly shows pixels where the aerosol optical thickness of 0.5 was retrieved.

The Olympic Peninsula and Bangladesh scenes were simulated using the MODTRAN radiation transfer model with rural aerosol and mid-latitude summer atmospheres. A calibration error of 2% and sensor noise model 3 were used for simulation. The Olympic Peninsula scene is illustrated in this document. Figure 11a is the original TERCAT scene provided by the IPO. Figure 11b is the “true” optical thickness simulated using MODTRAN on top of the scene. The retrieval at the 600 m GIFOV is shown in Figure 11c and at the horizontal cell size of 10.2 km in Figure 11d. The accuracy results for the aggregated product were better than our specified requirement over land of $0.05 + 0.2\tau$ and are presented in Table 6. The precision results did not quite meet our specification (again, $0.05 + 0.2\tau$) due to the unrealistic “wedge” of aerosols simulated. This retrieval was performed to include as many pixels as possible in the retrieval.

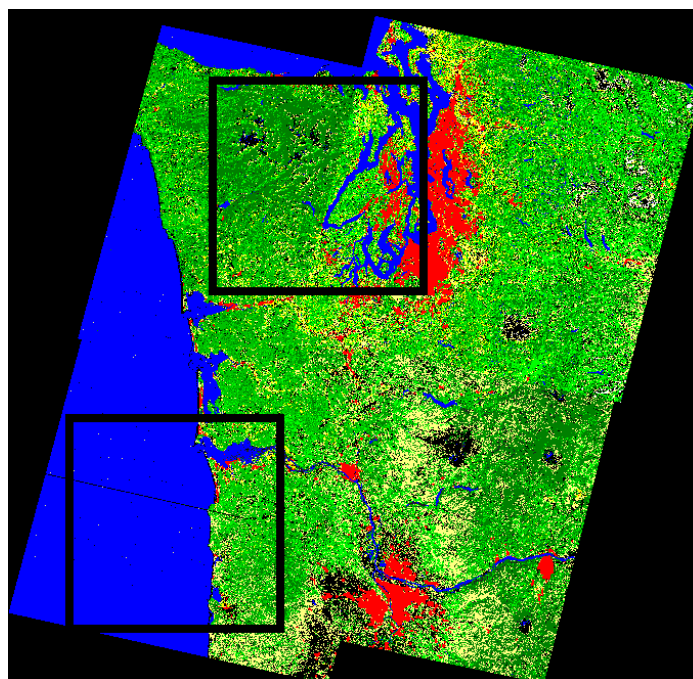


Figure 11a. TERCAT scene of the Olympic Peninsula provided by the IPO. This simulation is on the top subscene.

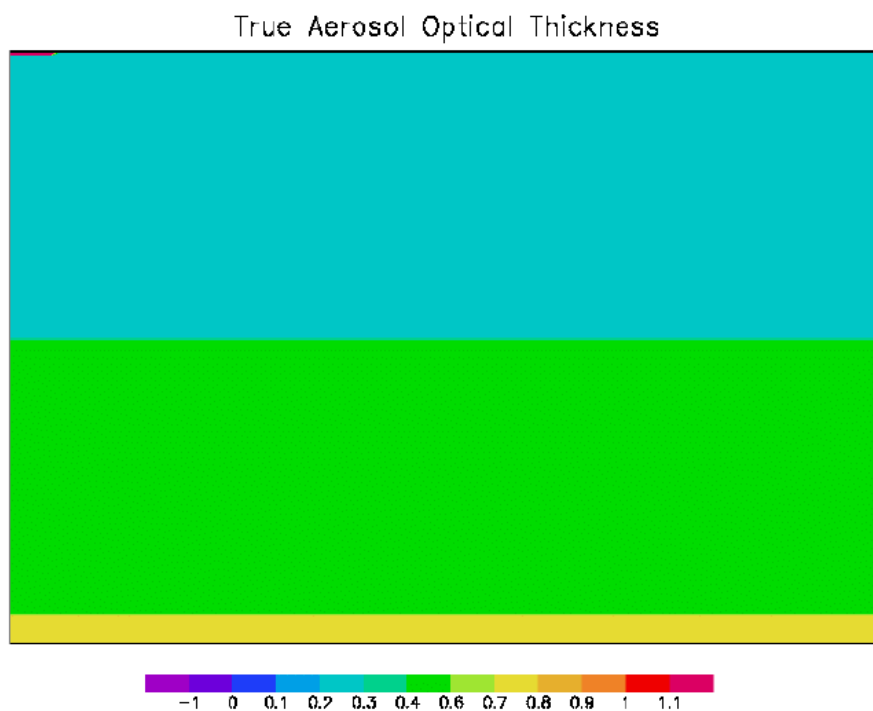


Figure 11b. The “true” simulated optical thickness.

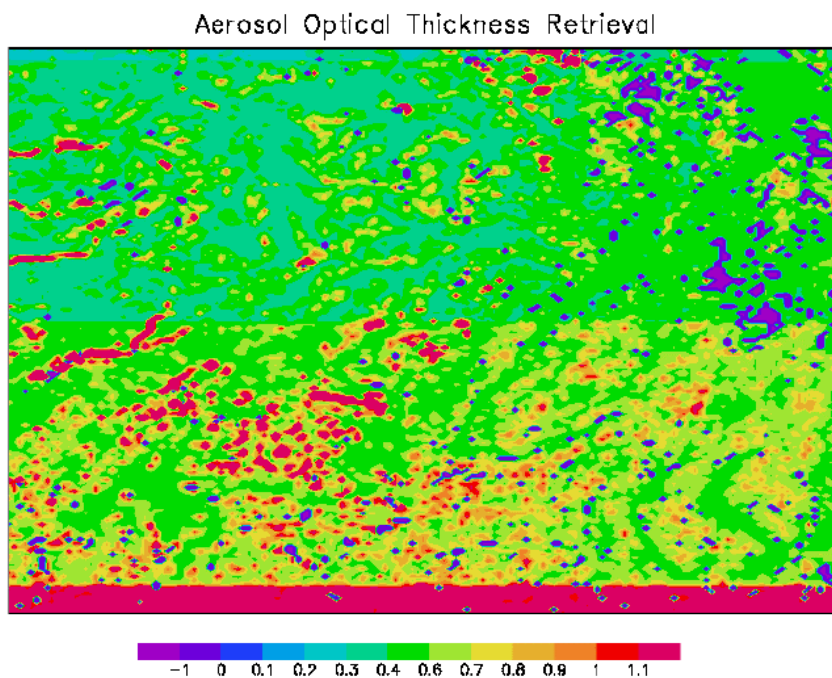


Figure 11c. Optical Thickness Retrieval at 600 m GIFOV.

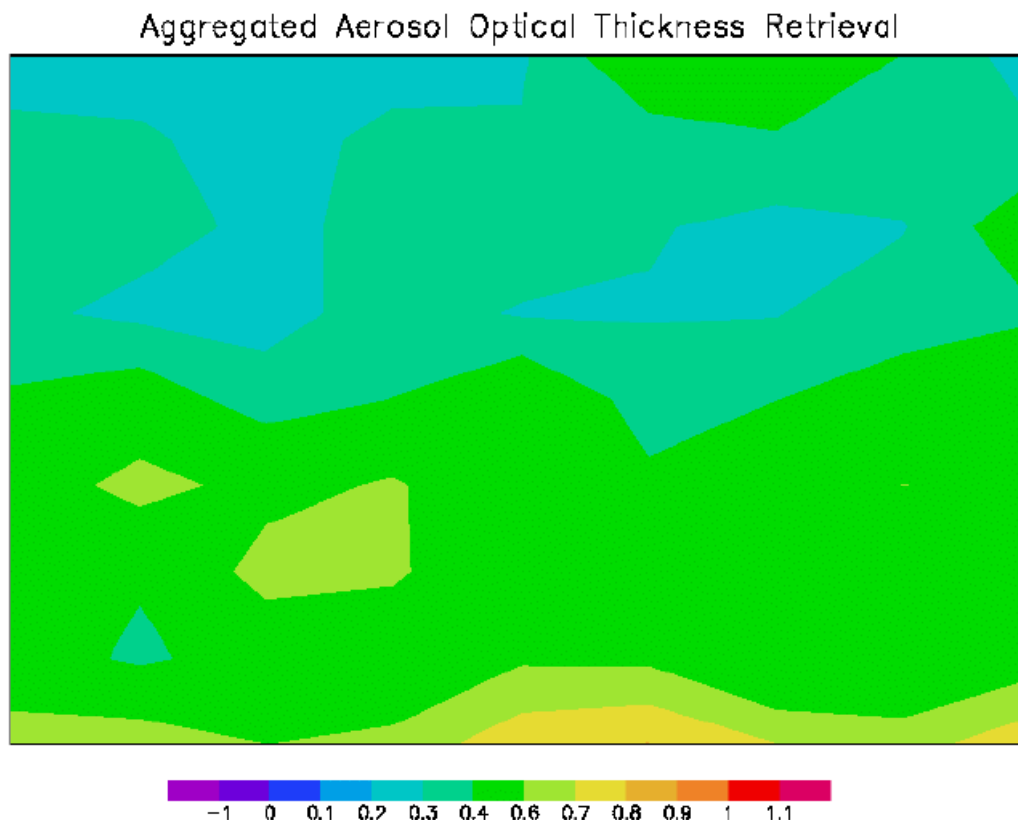


Figure 11d. Optical Thickness Retrieval at 10.2 km Horizontal Cell Size. Note: Most errors arise from the artificial aerosol optical thickness boundaries produced in the synthetic simulation.

3.4.2 Calibration Errors

The calibration requirements of the algorithm are being analyzed. Requirements for VIIRS baseline bands 2-6 have been derived using the VIIRS simulated orbital viewing geometries and the 6S radiative transfer code with aerosol optical depth perturbations of 0.03, the allowed accuracy error stated in the SRD [Y-1] for optical thicknesses over the ocean. The radiance and reflectance requirements are equivalent, as the reflectance differs from the radiance only by a multiplier. The calibration requirements for typical global mean aerosol optical depths of 0.20 are given in Table 6. The proposed VIIRS sensor is specifying a 2% absolute calibration requirement for the visible bands.

The aerosol size parameter was also examined using 6S. By definition in the SRD [Y-1], the aerosol size parameter must be calculated from two bands that are more than 200 nm apart, and less than 50 nm wide. It was found that the relative calibration errors between the bands cannot exceed 8 percent. This value was derived from a spreadsheet calculation of size parameter assuming an optical thickness of 0.1 in bands 5 and 6. The true value of the size parameter was 0.

Analyses have also been performed using the algorithm itself to determine the sensitivity of the algorithm to errors in the input reflectances. This analysis determined that the calibration accuracy required by the algorithm to meet the SRD requirements becomes stricter with increasing optical depth (i.e., brighter pixels).

Table 6. Aggregated Optical Thickness Retrieval Results for Olympic Peninsula Scene at HCS

True Value	Accuracy	Precision	Specification
0.288	0.036	0.071	0.108
0.355	0.036	0.228	0.121
0.400	0.120	0.144	0.130
0.559	0.139	0.039	0.162

Table 7. Calibration Requirements for Typical Global Mean Aerosol Optical Depth of 0.20

Band	Allowed Calibration Errors	Required Calibration on Sensor
0.443 μm	2.5%	2.0%
0.488 μm	3.0%	2.0%
0.555 μm	4.4%	2.0%
0.645 μm	5.8%	2.0%
0.856 μm	7.5%	2.0%

3.4.3 Instrument Noise

The requirement for precision is driven by the sensor noise. Gaussian noise was simulated using a random number generator. This error was added to the input reflectances, with Signal-to-Noise Ratios (SNRs) varying from no noise added to noise with an SNR of 5. This test indicated that the accuracy was not significantly affected by noise. The precision, however, was affected. As SNR decreased (noise increased) the precision decreased (standard deviation increased) linearly.

SBRS has developed a model of the proposed VIIRS sensor which can be applied to input radiances to simulate the effects of noise on the algorithm. We specified a noise/calibration requirement for the sensor, and SBRS has predicted the performance of the sensor they are developing to meet the algorithm requirements. A sensor model representing the sensor performance expected by SBRS has been provided and applied to the ocean simulated scene. A calibration error of 2% was also used to perturb the radiances. A summary of the results is shown below in Table 8.

Table 8a. AOT and APS Performances using SBRS Predicted Sensor Model

AOT(550nm) = 0.05				
Band (microns)	Truth	Specification	Accuracy	Precision
0.49	0.05	0.02	0.01	0.01
0.56	0.05	0.02	0.01	0.00
0.68	0.05	0.02	0.00	0.00
0.87	0.05	0.02	0.01	0.01
1.61	0.04	0.02	0.00	0.00
2.25	0.03	0.02	0.01	0.01
3.70	0.03	0.02	0.01	0.01

Table 8b.

AOT(550nm) = 0.20				
Band (microns)	Truth	Specification	Accuracy	Precision
0.488	0.21	0.02	0.02	0.01
0.555	0.20	0.02	0.01	0.01
0.682	0.19	0.02	0.01	0.01
0.865	0.18	0.02	0.01	0.01
1.61	0.16	0.02	0.01	0.00
2.25	0.14	0.02	0.01	0.01
3.7	0.12	0.02	0.01	0.01

Table 8c.

AOT(550nm) = 0.75					
Band (microns)	Truth	Spec. Acc.	Accuracy	Spec. Prec.	Precision
0.49	0.77	0.04	0.04	0.03	0.02
0.56	0.75	0.04	0.02	0.02	0.02
0.68	0.72	0.04	0.02	0.02	0.02
0.87	0.68	0.03	0.01	0.02	0.02
1.61	0.60	0.03	0.01	0.02	0.02
2.25	0.52	0.02	0.03	0.02	0.01
3.70	0.44	0.02	0.01	0.02	0.01

Table 8d.

AOT(550nm) = 1.50					
Band (microns)	Truth	Spec. Acc.	Accuracy	Spec. Prec.	Precision
0.49	1.76	0.11	0.11	0.05	0.04
0.56	1.48	0.09	0.09	0.04	0.02
0.68	1.12	0.06	0.05	0.03	0.01
0.87	0.74	0.04	0.03	0.02	0.01
1.61	0.20	0.02	0.00	0.02	0.00
2.25	0.08	0.02	0.02	0.02	0.00
3.70	0.02	0.02	0.01	0.02	0.00

Table 8e.

Ångström Exponent (672nm and 865nm)				
AOT	Truth	Specification	Accuracy	Precision
0.05	0.21	0.30	0.27	0.13
0.20	0.21	0.30	0.09	0.06
0.75	0.21	0.10	0.05	0.02
1.50	1.97	0.10	0.07	0.01

Table 8 shows the results of the application of the SBRS sensor model to a the simulated ocean scene described in section 3.4.1. The optical thickness was retrieved in 7 bands. The true value of optical thickness for each band is given. Four values of optical thickness within the specified retrieval range were used: 0.05, 0.20, 0.75, and 1.50. The maritime aerosol model was used for the three lower optical thickness simulations, and the biomass aerosol model was used for the 1.50 optical thickness simulation. The specification for accuracy ($0.02 \tau < 0.5$, $0.07\tau - 0.015 \tau > 0.5$) and precision ($0.02 \tau < 0.5$, $0.02\tau + 0.01 \tau > 0.5$) for each value of optical thickness and each band is listed. The tables show clearly that for each band the specification is achieved for accuracy and precision. The Ångström exponent was also retrieved for these simulations for each value of optical thickness using the 672 nm and 865 nm bands. The retrievals at 0.2, 0.75, and 1.50 are within the specification for those value of optical thickness. The retrieval of the 0.05 scene does not meet our specification. The Ångström exponent retrieval is not guaranteed to meet specification at low values of optical thickness (≤ 0.05).

3.4.4 Band Selection

The earlier aerosol retrieval is based on a single-channel technique (e.g., Griggs, 1975). Stowe *et al.* (1997) proposed the use of the two-channel technique, $0.63 \mu\text{m}$ and $1.6 \mu\text{m}$ (or $0.83 \mu\text{m}$), to replace the existing one-channel ($0.63 \mu\text{m}$) technique for adding the capability of aerosol size parameter retrieval over ocean from AVHRR measurements. Their primary idealized (assuming deep calm ocean) forward simulations imply that the $1.6 \mu\text{m}$ channel works better than the $0.83 \mu\text{m}$ channel because of the relative complex water vapor absorption in the $0.83 \mu\text{m}$ band. Stowe *et al.* (1997) also pointed out that “the AVHRR instrument is not the optimum instrument for making aerosol measurements” because there is no onboard calibration for its reflectance measuring channels. They believe remote sensing of aerosol physics and chemical properties should be improved beyond AVHRR’s capabilities with the development of spaceborne multispectral imaging spectrometers.

Our algorithm uses as many bands as possible for accurate aerosol optical depth and size parameter retrievals. The exact placement of the bands is flexible, as the bands used should only be outside of the absorption window with a width sufficiently small so as not to smooth the spectral variations. The derived size parameter may be used to make a better determination of optical thickness by helping to determine the most accurate aerosol model to use. The water vapor and ozone absorption that is present in the VIIRS baseline bands can be corrected using ozone and total precipitable water information from VIIRS itself and NCEP/NOGAPS model data. For the optical thickness algorithm the visible bands are used to calculate the aerosol contribution to the measured reflectances. The surface contribution is estimated from the near-IR

bands. Bands 9 (2.25 μm) and 10 (3.7 μm) are used to find dark, vegetated pixels required to retrieve optical thickness over land. The 2.25 μm band is much more sensitive to dense, dark vegetated pixels than the 1.6 μm channel, as the reflectance at 2.25 μm is much lower than that in 1.61 μm in the presence of vegetation. The 2.25 μm band is also significantly less sensitive to aerosols than the 1.61 μm band since it is at a longer wavelength and thus not scattered by aerosols. The 2.25 μm band is included in the VIIRS design for dark pixel detection for the aerosol optical thickness over land retrieval.

The Ångström exponent must be calculated from the retrieved optical thicknesses of two bands separated by at least 200 nm. On the proposed VIIRS, there are 17 possible band combinations. Studies of the effective radius have shown that a better effective radius can be retrieved using an Ångström exponent retrieved using the 0.670 and 1.60 μm bands than the 0.670 and 0.870 μm bands due to the larger sensitivity to larger particles in the longer wavelengths.

3.4.5 Other

A forward technique has been used to perform sensitivity studies on ancillary data. This technique applies the 6S radiative transfer model to the simulated VIIRS orbital viewing geometries. The surface was assumed to be ocean in one set of runs and homogeneous land in another set. The results are summarized in Tables 8 and 9.

Over oceans, the typical aerosol optical thickness of 0.2 is used. The aerosol optical thickness precision is affected by uncertainties in the ancillary data and equals ± 0.0064 or $\pm 1.24\%$ of the reflectance for typical uncertainties in the ancillary data (refer to Table 8). It appears these uncertainties are independent of the mean aerosol optical depth; therefore, for aerosol optical thickness of less than 0.05 the precision level will be greater than or equal to $\pm 14\%$ of the mean values. The precision level is dominated by uncertainties in wind velocity, which gives rise to uncertainties in the coverage by whitecaps. As a first-order approximation, we expect all bands in all orbits will have values for precision of the same order of magnitude. To test this, we examined band 6 (0.8585 μm) and found the uncertainty in aerosol optical thickness retrieval is ± 0.0058 , or about the same as band 5 (0.645 μm). It is important in deriving optical thickness to remove regions of sun glint, and this was done for this analysis. If sun glint is not removed, the precision of the measurements drops markedly. The reflectance uncertainty due to water vapor applies only to the 620-670 nm band originally proposed for the VIIRS design that has water vapor absorption. In the current VIIRS design, a 662-692 nm band is proposed and uncertainties arising from total precipitable water become negligible. In conclusion, it appears that threshold aerosol optical thickness precision can be met over oceans with the expected ancillary data uncertainties.

Over land, threshold precision requirement is ± 0.2 . Simulations using the 6S code on the 1:30 p.m. orbit give precisions of 0.053 or better over land for aerosol optical thicknesses less than 2. According to the MODIS ATBD (Kaufman and Tanré, 1996), the uncertainty in reflectance for these bands will be between 0.5% and 1% and is the major contributor to reducing precision. In conclusion, it appears that threshold aerosol optical thickness precision can be met over land as well with the expected ancillary data uncertainties.

Table 9. Ancillary Data Required by the Optical Thickness and Size Parameter Algorithm

Ancillary Data Requirements Effects on Aerosol Optical Depth Precision Band 5; 1:30 PM Orbit Over Oceans			
Ancillary EDR	Ancillary EDR Uncertainty	Reflectance Uncertainty (1 s. d.)	Aerosol Optical Depth Uncertainty (1 s. d.)
Wind velocity	± 1 m/s	$\pm 1.08\%$	± 0.0056
Wind direction	$\pm 20^\circ$	$\pm 0.46\%$	± 0.0024
Total precipitable water	± 0.2 cm	$\pm 0.14\%$	± 0.0008
Total column ozone	± 0.015 cm	$\pm 0.36\%$	± 0.0018
Ocean chlorophyll concentration	± 0.03 mg/m ³	$\pm 0.11\%$	± 0.0005
Surface pressure	± 10 mb	Negligible	Negligible
Platform pointing	± 5 pixels	Negligible	Negligible
RSS totals		$\pm 1.24\%$	± 0.0064

Table10. Ancillary Data Required by the Optical Thickness and Size Parameter Algorithm for a Single Pixel

Ancillary Data Requirements Effects on Aerosol Optical Depth Precision Band 5; 1:30 PM Orbit Over Land For a Single Pixel			
Ancillary EDR	Ancillary EDR Uncertainty	Reflectance Uncertainty (1 s. d.)	Aerosol Optical Depth Uncertainty (1 s. d.)
Surface reflectance	± 0.01	$\pm 6.2\%$	± 0.032
Total precipitable water	± 0.2 cm	$\pm 0.14\%$	± 0.0008
Total column ozone	± 0.015 cm	$\pm 0.36\%$	± 0.0018
Surface pressure	± 10 mb	Negligible	Negligible
Platform pointing	± 1 pixel	Scene dependent	Scene dependent
RSS totals		$\pm 6.24\%$	± 0.0322

In our simulation here, a single pixel is used. In the actual retrievals of aerosol optical thickness over land, as many as 100 pixels may be used to form a 10 by 10 km mean. In this case, uncertainties in surface reflectance tend to cancel out, so the threshold requirement for precision may be improved by about a factor of 20 by the aggregation of pixels. In the report for VIIRS aerosol TBDs/TBRs, we proposed the use of a formula making the requirements of accuracy and precision dependent on optical thickness and wavelength, such as $\Delta\tau = \pm 0.05 + 0.20\tau$ (over land) and $\Delta\tau = \pm 0.01 + 0.1\tau$ (over ocean). The proposed change would remove the more strict requirements on brighter scenes to make the requirements uniform for all scenes. It also allows the size parameter (α) to be determined to within the threshold measurement accuracy of 0.3 for all aerosol optical thicknesses. Finally, the aerosol scientific community uses a similar function approach to accuracy (or precision) specifications for MODIS, MERIS, and AGI.

Pixel alignment may become an issue for aerosol retrieval when two wavelength bands are assumed to be looking at the same location to deduce size parameter, but are not. No error will occur for a perfectly constructed instrument. In reality, one wavelength band may be systematically pointing at a different location than the other wavelength band. If the underlying surface has a uniform reflectance, then only small errors in determination of aerosol size distribution can be expected because the spatial scales upon which size distribution vary are much larger than the pixel size. Only in the case where the underlying surface has rapid variations in surface might it be interpreted as arising from aerosols and give rise to incorrect determinations of the aerosol size distribution. To test this idea, a radiative transfer spreadsheet was run for the case where adjacent pixels had contrasts in surface reflectance of 0.05, 0.1, 0.15, and 0.2 for a wide range of aerosol size distributions. The results are presented in Table 10, where the allowable pixel misalignments are given in units of pixels such that the size parameter accuracy of 0.3 will be maintained. The results are functions of adjacent pixel contrasts and of alpha.

Table 11. Calculations of the effect of Pixel Reflectance Differences on Ångström Exponent

α	Pixel Reflectance Differences			
	0.05	0.10	0.15	0.20
-1	0.68	0.34	0.23	0.17
0	0.78	0.39	0.26	0.20
1	0.88	0.44	0.29	0.22
2	1.14	0.57	0.38	0.29
3	1.82	0.91	0.61	0.46

The following conclusions can be made: 1) Large pixel-to-pixel contrasts drive alignment requirements; 2) the next driver is the alpha value (lower values require better alignments); and 3) the results are only weakly dependent upon aerosol optical depth. For the 20 cases shown in Table 9 the mean alignment requirement is about 0.55 pixels. However, the pixel alignment requirements are less stringent for aerosols because the average contrast between adjacent pixels is of the order of 0.05 or less. In short, aerosols are not driving the alignment requirements of VIIRS. It is more likely land surface classification will be a VIIRS alignment driver. In the current analysis, VIIRS bands 4 ($\lambda=0.556 \mu\text{m}$) and 5 ($\lambda=0.645 \mu\text{m}$) were used, but the results are not expected to differ much if other bands are used.

We would expect that the error of aerosol retrieval introduced from mapping uncertainties is similar to the above alignment error as a first-order approximation because the mapping error is very similar to the alignment error. We know that the approximate lower limit of horizontal spatial scales upon which there is obvious difference in tropospheric aerosol properties is close to mapping error and should be between these two values to avoid rapid variations in aerosol properties and in the reflectance of the underlying surface. It is possible to achieve the threshold mapping errors (4 km) proposed in the SRD [Y-1], but the objective (1 km) may be difficult.

3.5 PRACTICAL CONSIDERATIONS

3.5.1 Numerical Computation Considerations

The aerosol retrieval algorithms over land and ocean are based on the LUT technique. The linear interpolation on the LUTs is used to derive optical thickness from grid values on the table. Extrapolation of the LUT is not permitted to ensure reasonable physical meaning. The error introduced from the interpolation is much less than that from the uncertainty in the surface reflectance, aerosol model, and wind speed.

3.5.2 Programming and Procedural Considerations

The procedural outline has been described in Section 3.1.

3.5.3 Configuration of Retrievals

To avoid "hard-wiring" specific values into the operational software, a retrieval configuration file can be adopted. The file would store numerical values of adjustable parameters used within the retrievals, such as the thresholds establishing whether a successful retrieval occurs.

3.5.4 Quality Assessment and Diagnostics

We may introduce a quality assurance (QA) flag for VIIRS aerosol products over land and ocean to reflect the quality of aerosol parameters retrieved by our algorithms. The QA flag will be stored in a 10 by 10-km grid, which is the same as the cell size for aerosol optical thickness retrieval. The number of cloud-free pixels in the 10 by 10-km cell size, the standard deviation calculated using the percentiles, and the surface reflectance at 2.1 μm may be considered part of the quality assurance.

3.5.5 Exception Handling

Aerosol retrieval applicability is tested on the pixel level. If a pixel is found to be unusable or contaminated according to a certain test, the remaining tests are not performed and the pixel is discarded.

3.6 ALGORITHM VALIDATION

3.6.1 Pre-Launch Validation Studies

The pre-launch research algorithm will be verified using AVHRR, SeaWiFS, and simulated VIIRS data. Optical depths derived from 1993 AVHRR data were compared to AERONET (see the next section for more on AERONET) sun-photometer observations from the same time period over the eastern United States and Brazil. These results are illustrated in Figures 12 and 13. These preliminary results indicate good agreement, but more studies with larger samples are required to demonstrate that the goals of the measurement accuracy are being met.

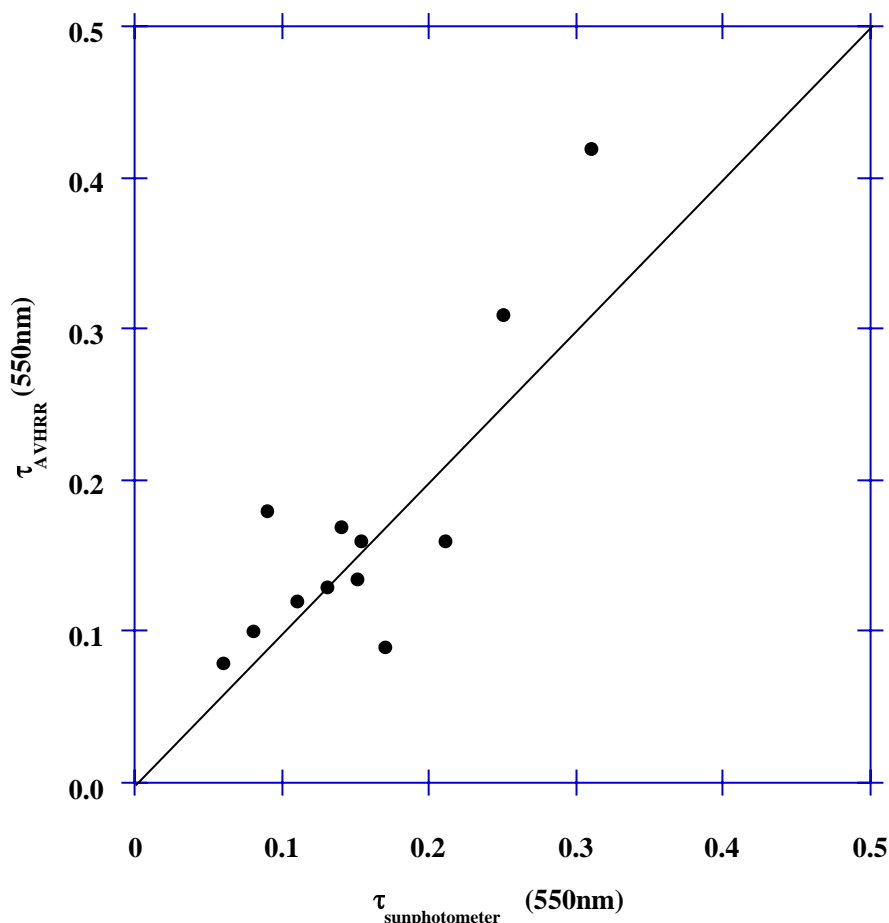


Figure 12. Comparison of retrieved optical depth using AVHRR data and the dark target approach with measured optical depth from AERONET in August 1993 over the Eastern United States.

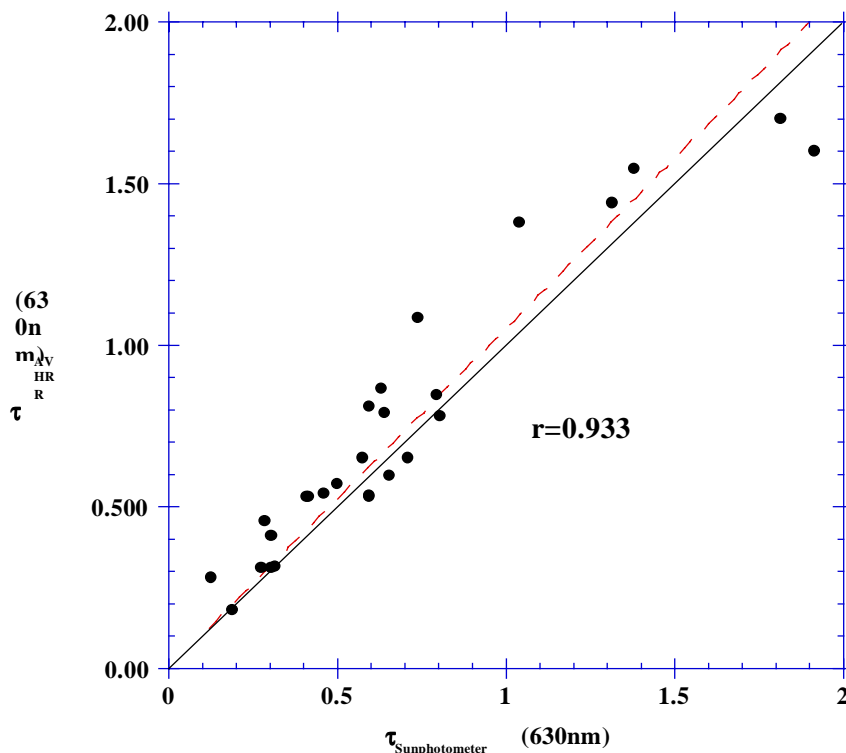


Figure 13. Comparison of retrieved optical depth using AVHRR data and the dark target approach with measured optical depth from AERONET in 1993 over Brazil.

AVHRR and AERONET data for the September–December 1997 period were used with 6S to improve the retrieval algorithm over land. The main improvement to the algorithm consists of including larger land areas where it can be applied by estimating the surface reflectance in the red band (0.67 μm) from the middle infrared band (3.75 μm). Figure 14 shows the empirical relation between the red and mid-infrared reflectances derived from AVHRR data for November 1997.

An algorithm combining AVHRR data with SeaWiFS data was developed by Eric Vermote for aerosol optical thickness retrieval over land and ocean. AVHRR data was used to generate a monthly composite of reflectance in the 3.75 μm band and a snow map. Then the AVHRR was read for every noncloudy, dark, vegetated SeaWiFS pixel. A pixel was determined to be dark by the Enhanced Vegetation Index (EVI), which is resistant to aerosol contamination. The 3.75 μm reflectance was then used to compute the SeaWiFS surface reflectance in the red and blue bands. The SeaWiFS top of the atmosphere measured reflectance in the red and blue band was then inverted to obtain the aerosol optical thickness in these bands.

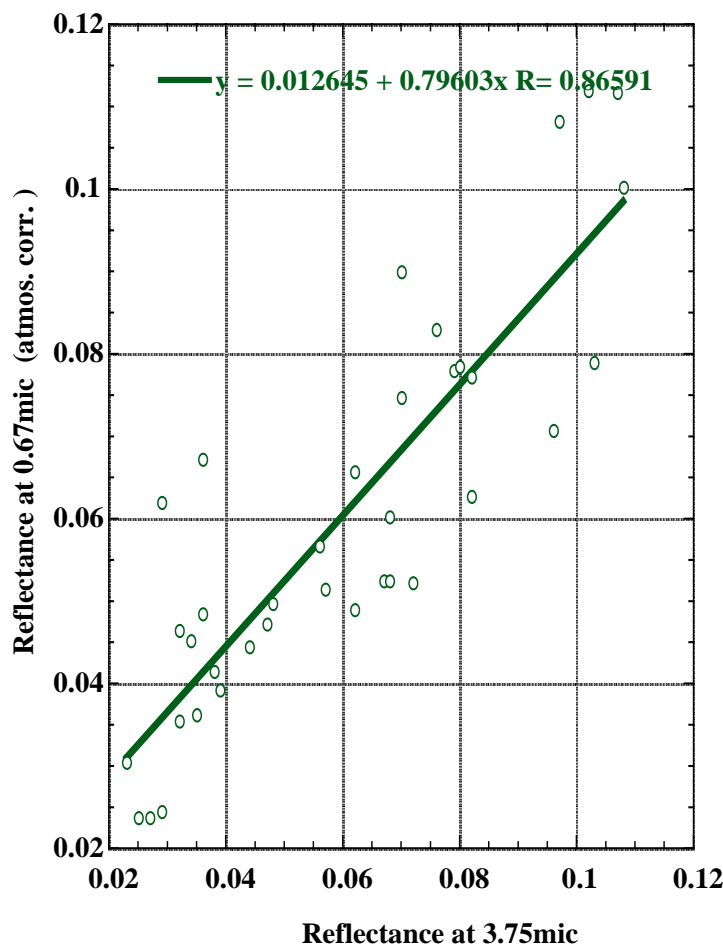


Figure 14. Empirical relation between the red (0.67 μm) and mid-infrared (3.75 μm) reflectances derived from AVHRR data for November 1997.

Three months of SeaWiFS data were processed using this software and were evaluated by comparison to AVHRR retrievals and sun-photometer measurements. An example of aerosol optical thickness retrieved over land from AVHRR and SeaWiFS data for September 27, 1997 is presented in Figure 15.

The availability of multiple visible bands in SeaWiFS makes it appropriate to determine aerosol characteristics by retrieving the optical thickness at different wavelengths. We initiated an effort in this direction, where optical thickness retrieval from SeaWiFS data is performed in the red and blue bands as shown in Figure 16. Retrievals of the Ångström exponent have also been performed using SeaWiFS data (see Figure 17).

In-house work to simulate VIIRS data used both the MODTRAN and the 6S codes. These simulated scenes will have known aerosol optical depths so that comparing the derived aerosol optical depths to the known aerosol optical depths can test the algorithm. If they match, this provides evidence that the algorithm is working properly. If they fail to match, then it will be required to determine whether the problem is in the algorithm or in the simulated images.

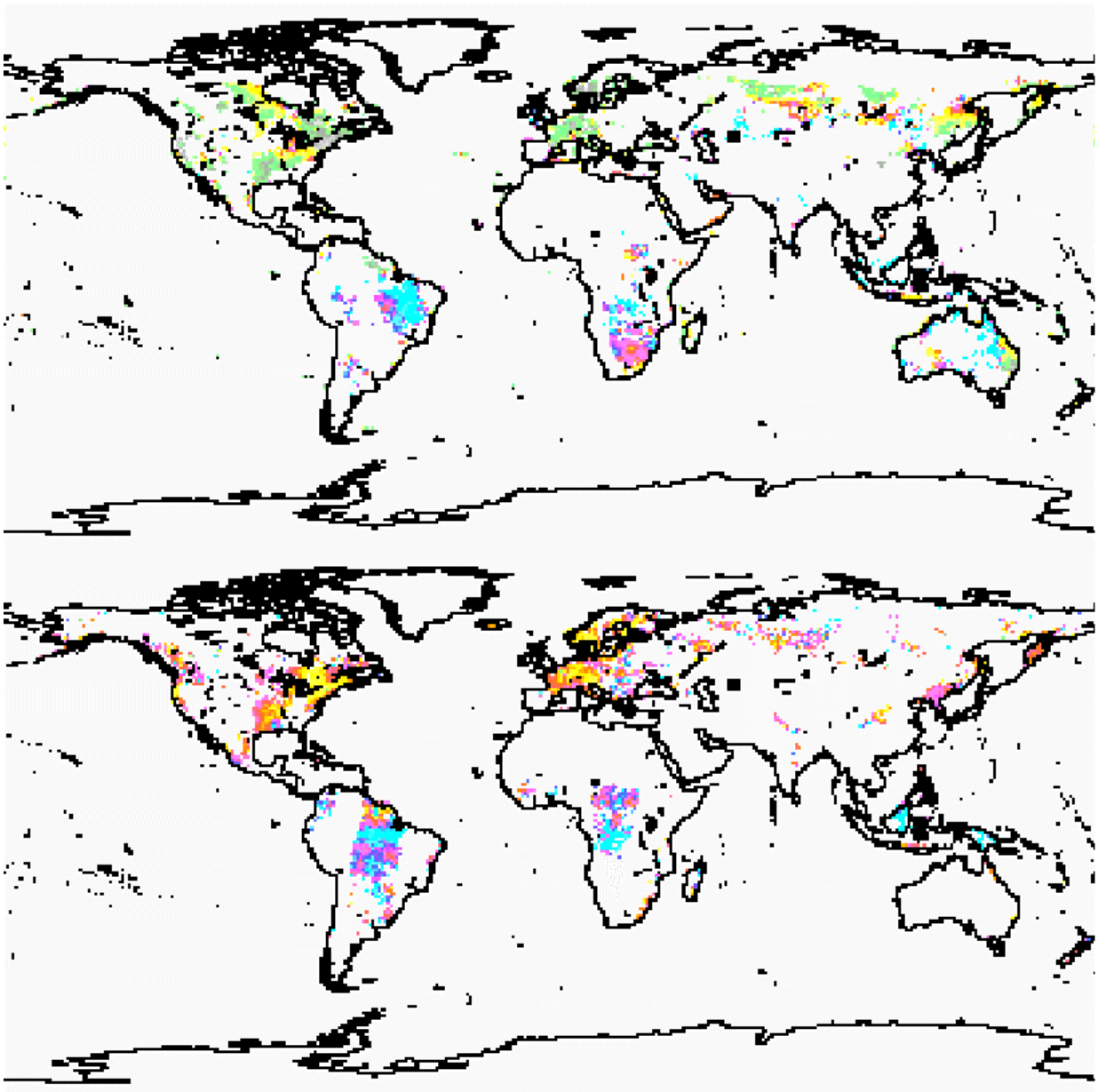


Figure 15. Aerosol optical thickness at 0.67 μm for 27-Sept.-97 derived from AVHRR (upper image) and SeaWiFS (lower image) data.

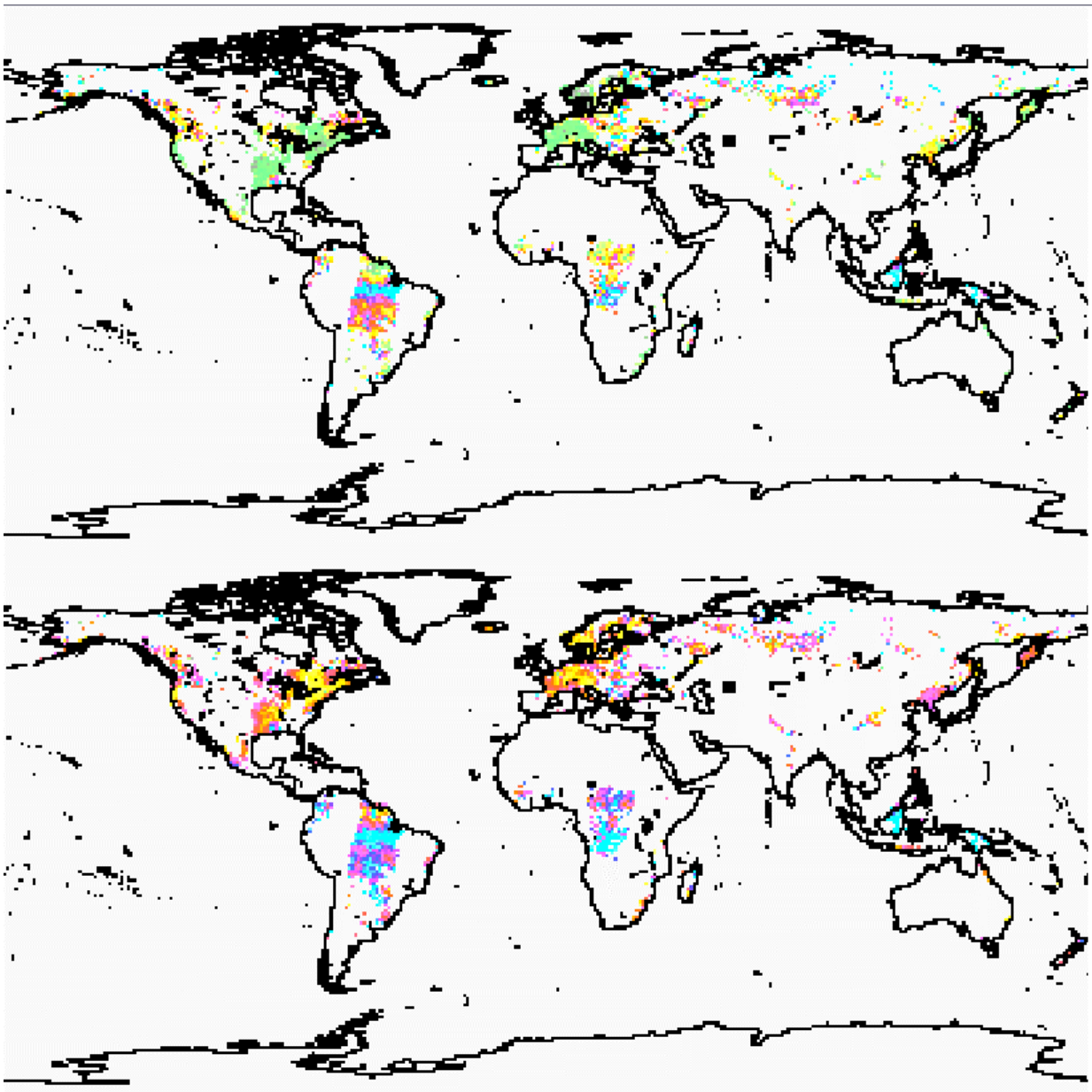


Figure 16. Aerosol optical thickness derived from SeaWiFS data for 27-Sept.-97 at 0.443 μm (upper image) and 0.67 μm (lower image).

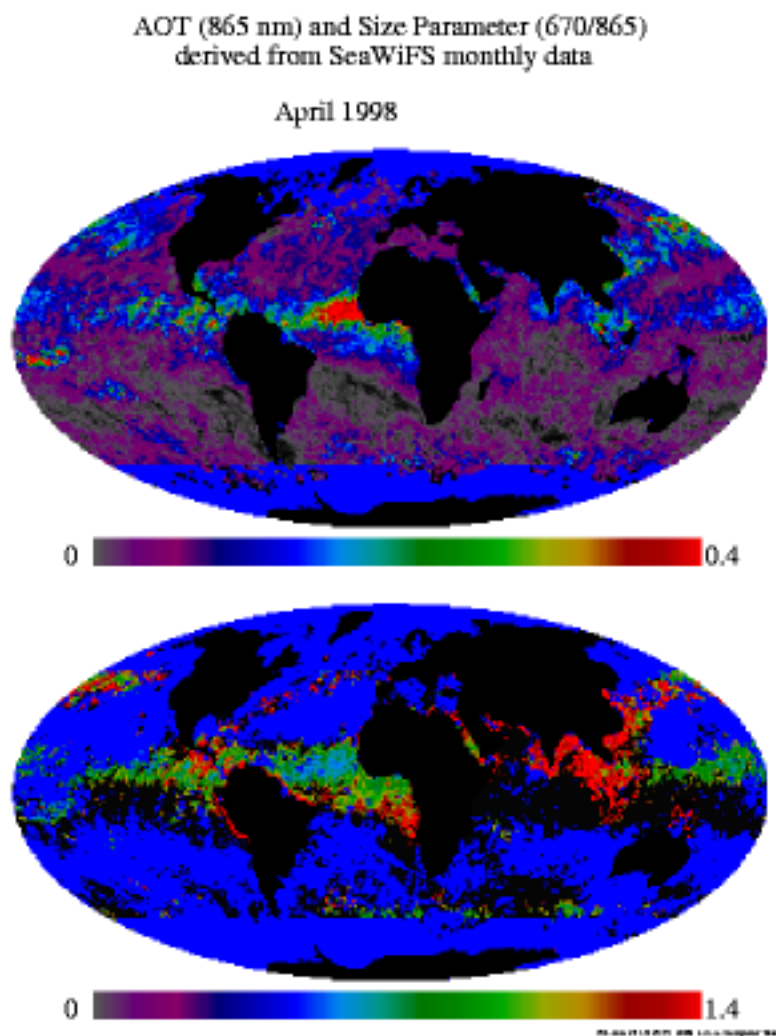


Figure 17. Retrieval of Aerosol Optical Thickness and Ångström Exponent using SeaWiFS data.

Finally, the IPO will provide us with a set of simulated images and the in-house validation process will be repeated on these images.

It is anticipated that the pre-launch operational algorithms will go through a similar testing procedure during the years 2000-2008.

3.6.2 Post-Launch Routine Ground-Based Observations

Post-launch routine ground-based observations can be made using AERONET, the International Aerosol Lidar Network, and any of the several miscellaneous techniques, including the diffuse/direct method, aureole meters, and polarization measurements.

AeRoNet

AeRoNet (Aerosol Robotic Network) is a network of ground-based sun-photometers established and maintained by Brent Holben of Code 923 of the NASA Goddard Space Flight Center and Tom Eck of Raytheon ITSS. The sun-photometers measure the spectral aerosol optical thickness and sky radiance. Data is sent via a satellite communication link from each remotely located CIMEL sun-photometer to Goddard Space Flight Center from sunrise to sunset, 7 days a week. The data is analyzed to give aerosol optical depths at several wavelengths and is then placed on the Internet with a delay of a few days.

By comparing the AeRoNet aerosol optical depths to the VIIRS aerosol optical depths, we can provide ground-truth observations to validate VIIRS. A large number of intercomparisons must be made to see if any systematic differences exist and if there are any trends in these differences. Because of the delay in the availability of the AeRoNet observations, it is not anticipated that the validation studies will be part of the operational code; rather, they will be a separate, off-line study. These measurements are expected to be the primary method of validating the VIIRS observations.

International Aerosol Lidar Network

The International Aerosol Lidar Network is a confederation of lidar investigators who take tropospheric and stratospheric measurements. These measurements are particularly useful for tracking volcanic dust clouds. They also offer an opportunity to validate the VIIRS aerosol optical depths.

Miscellaneous techniques

A number of miscellaneous techniques can be used to derive aerosol optical depths. They include aureole meters, measurements of location of polarization neutral points, and the direct/diffuse method using pyrheliometers and pyranometers. Most of these observations are only made occasionally, but they may offer opportunities for intermittent comparison to the VIIRS aerosol optical thicknesses.

3.6.3 Post-Launch Special Field Experiments

Many of the present satellite observations are augmented by special field campaigns to provide ground-truth data for the satellite-derived measurements. Although the NPOESS project does not yet have formal plans for such experiments, it is anticipated that they will be required for calibration purposes. The VIIRS aerosol optical thickness and size distribution measurements could be validated using sun-photometer and lidar observations. Suspended matter determinations might be checked by Fourier transform interferometer measurements, *in situ* chemical analyses, and dustsondes. The details of these campaigns (timing, location, instrumentation, aircraft use, etc.) will not be determined solely by the aerosol validation requirements, so these experiments will not be further discussed here.

3.6.4 Post-Launch Satellite-Based Intercomparisons

VIIRS-derived aerosol optical depths may be validated by comparing them with aerosol optical depths derived by other satellite sensors, such as MODIS. It is not clear what sensors will be flying contemporaneously with VIIRS after the year 2008. The basic intercomparison technique involves four steps: 1) identification of locations where both sensors fly over at nearly the same time; 2) extraction of data for storage in an intercomparison archive; 3) analysis of the differences between the measurements; and 4) communication of the results to the appropriate people so that proper corrective actions can be taken if needed. It is possible that the intercomparison procedure could be fully automated and put in the operational code, but it is more likely that it will involve human intervention and judgment to understand the results.

Another validation method for the routine VIIRS aerosol retrieval algorithm is the use of different retrieval algorithms, but still using the VIIRS data. One example of this approach would be the use of the path radiance method of Wen et al. (1999) that allows aerosol optical depth retrievals over land without making assumptions about the spectral variations in surface reflectance. The method appears to work best for near-nadir views where the complication of BRDF variations are minimized. Comparisons of the aerosol optical thicknesses derived from the routine algorithm and the path radiance algorithm could be used to validate the routine observations.

3.7 ALGORITHM DEVELOPMENT SCHEDULE

Enhancements of the aerosol optical thickness and particle size parameter algorithm were implemented during the winter of 1999/2000. Additional aerosol models were used for optical thickness determination, and suspended matter information was used to choose the most representative aerosol model. The effective radius algorithm was developed using AeRoNet data.

The aerosol optical thickness and particle size parameter algorithms are 90% complete for CDR. During Phase 2, details of the algorithm will be refined, and enhancements to extend the retrievals to brighter pixels will be added. We will take advantage of the free validation offered by the MODIS launch, as our proposed VIIRS and MODIS share many of the same bands. The MODIS data will facilitate the refinement of the VIIRS aerosol algorithm.

4.0 ASSUMPTIONS AND LIMITATIONS

4.1 ASSUMPTIONS

The following assumptions are made with respect to the aerosol retrievals described in this document:

- (1) Aerosol particles are homogeneous spheres.
- (2) A horizontally homogeneous atmosphere applies to each horizontal cell size of aerosol products.

4.2 LIMITATIONS

Limitations applying to our aerosol retrieval are:

- (1) Retrievals will only be specified over regions with dark water and dark vegetation surfaces.
- (2) Retrievals will be performed under clear conditions.
- (3) Retrievals will only be specified for solar zenith angles larger than 70°.

5.0 REFERENCES

- Charlson, R. J., S. E. Schwartz, J. M. Hales, R. D. Cess, J. A. Coackley Jr., J. E. Hansen, and D. J. Hofman (1992). Climate forcing of anthropogenic aerosols. *Science*, 255, 423-430.
- Cox, C., and W. Munk (1954). Statistics of the sea surface derived from sun glitter. *J. Mar. Res.*, 13, 198-208.
- Eck, T. F., B. N. Holben, J. S. Reid, O. Dubovik, A. Smirnov, N. T. O'Neill, I. Slutsker, and S. Kinne, 1999. Wavelength dependence of the optical depth of biomass burning, urban, and desert dust aerosols. *J. Geophys. Res.*, 104D, 31333-31349.
- Ferrare, R. A., R. S. Fraser, and Y. J. Kaufman (1990). Satellite remote sensing of large-scale air pollution: Measurements of forest fires smoke, *J. Geophys. Res.*, 95, 9911-9925.
- Geogdzhayev, I. V. and M. I. Mishchenko, 1999. Preliminary Aerosol Climatology for the Period of NOAA-9 Observations (<http://gacp.giss.nasa.gov>)
- Griggs, M. (1975). Measurements of atmospheric aerosol optical thickness using ERTS-1 data, *J. Air pollut. Control Assoc.*, 25, 622-626.
- Hansen, J. E., and A. A. Lacis (1990). Sun and dust versus greenhouse gases: An assessment of their relative roles in global climate change. *Nature*, 346, 713-719.
- Hsu, N.C., J.R. Herman, J. Gleason, O. Torres, and C.J. Seftor. Satellite detection of smoke aerosols over a snow/ice surface by TOMS. To be submitted to *Geophys. Res. Lett.* In 1998.
- Intergovernmental Panel on Climate Change (IPCC) (1994). Radiative Forcing of Climate Change. Edited by B. Bolin, J. Houghton, and L. G. M. Filho, UNEP, World Meteorol. Organ., Geneva.
- Kaufman, Y. J., R. S. Fraser, and R. A. Ferrare (1990). Satellite measurements of large-scale air pollution methods, *J. Geophys. Res.*, 95, 9895-9909.
- Kaufman, Y. J., and D. Tanré (1996). Algorithm for Remote Sensing of Tropospheric Aerosol from MODIS, <http://eosps.gsfc.nasa.gov/atbd/modistables.html>.
- Kaufman, Y. J., D. Tanré, L. A. Remer, E. F. Vermote, A. Chu, and B. N. Holben (1997). Operational remote sensing of tropospheric aerosol over land from EOS moderate resolution imaging spectroradiometer. *J. Geophys. Res.*, 102, 16971-16988.
- Kaufman, Y. J., A. E. Wald, L. A. Remer, B. Gao, R. Li, and L. Flynn (1997). The MODIS 2.1- μm Channel-Correlation With Visible Reflectance for Use in Remote Sensing of Aerosol. *IEEE Trans. on Geoscience and Remote Sensing*, 35, 1286-1298.

- King, M. D., D. M. Byrne, B. M. Herman, and J. A. Reagan (1978). Aerosol size distribution obtained by inversion of optical depth measurements. *J. Atmos. Sci.*, 35, 2153-2167.
- Koepke, P. (1984). Effective reflectance of oceanic whitecaps, *Appl. Opt.*, 23, 1816-1823.
- Mishchenko, M. I., A. A. Lacis, B. E. Carlson, and L. D. Travis (1995). Nonsphericity of dust-like tropospheric aerosols: Implications for aerosol remote sensing and climate modeling, *Geophys. Res. Letters*, 22, 1077-1080.
- Stowe, L. L., A. M. Ignatov, and R. R. Singh (1997). Development, validation, and potential enhancements to the second-generation operational aerosol product at the National Environmental Satellite, Data, and Information Service of the National Oceanic and Atmospheric Administration, *J. Geophys. Res.*, 102, 16,923-16,934.
- Tanré, D., M. Herman, and Y. J. Kaufman (1996). Information on aerosol size distribution contained in solar reflected spectral radiances. *J. Geophys. Res.*, 101, 19,043-19,060.
- Torres, d., P.K., Bhartia, J.R. Herman, Z. Ahmad, and J. Gleason (1998). Derivation of aerosol properties from satellite measurements of backscattered ultraviolet radiation: Theoretical basis. *J. Geophys. Res.*, 103, 17,099-17,110.
- Vermote, E., D. Tanré, J.L. Deuzé, M. Herman, and J.J. Morcette, 1997. 6S User Guide Version 2.
- Wen, G., S. Tsay, R. F. Cahalan, and L. Oreopoulos, 1999. Path radiance technique for retrieving aerosol optical thickness over land. *J. Geophys. Res.*, 104D, 31321-31332.